technologies

MDPI

Article

Transient Hydraulic Analysis for Pressure Surge Mitigation in Offshore Firewater Distribution Systems

Oana Stefania Damian [1], Radu Bosoanca [2] and Costel Ungureanu [2,*]

[1] ICEPRONAV Engineering SRL, 800025 Galati, Romania; oana.damian@icepronav.ro
[2] Faculty of Naval Architecture, "Dunarea de Jos" University of Galati, 800201 Galati, Romania; radu.bosoanca@ugal.ro
* Correspondence: costel.ungureanu@ugal.ro

Abstract

Hydraulic transients induced by rapid changes in operating conditions represent a major challenge in the design and safe operation of offshore Firewater systems. During emergency events, such as fire pump start-up or rapid valve operations, pressure waves may propagate throughout the distribution network, generating water hammer effects capable of compromising the integrity and reliability of critical safety equipment. This study investigates the transient hydraulic response of an offshore Firewater ring-main system installed on a Floating Production Storage and Offloading (FPSO) unit using a detailed numerical model developed in PIPENET Transient. Three representative emergency operating scenarios were analysed, including fire pump start-up, deluge valve closure, and monitor valve closure. For each scenario, the hydraulic response of the original system configuration was compared with a modified pressure-protection arrangement involving relocation of the check valve immediately downstream of the fire-pump discharge flange and reduction of the pressure safety valve (PSV) set pressure from 17.5 barg to 16.5 barg. The simulations enabled the identification of critical pressure locations, evaluation of transient pressure propagation, and assessment of the effectiveness of the proposed mitigation strategy. The results demonstrate that the modified pressure-protection arrangement reduces the governing system-level pressure peaks and attenuates transient pressure oscillations under the investigated operating conditions. The proposed engineering methodology provides practical support for the design verification and optimization of offshore Firewater systems and contributes to improving the operational safety and reliability of safety-critical piping networks.

Keywords: offshore firewater system; hydraulic transients; water hammer; pressure surge mitigation; pressure safety valve; PIPENET; FPSO

Check for updates

Academic Editor: Miklas Scholz

Received: 28 July 2026
Revised: 7 September 2026
Accepted: 9 September 2026
Published: 11 September 2026

Copyright: © 2026 by the authors. Licensee MDPI, Basel, Switzerland. This article is an open access article distributed under the terms and conditions of the Creative Commons Attribution (CC BY) license.

1. Introduction

Offshore oil and gas installations operate under particularly demanding safety conditions because large hydrocarbon inventories, high-pressure processing equipment, ignition sources and safety-critical systems are concentrated within restricted spatial arrangements. On Floating Production Storage and Offloading (FPSO) units, fires and explosions may produce cascading consequences involving personnel, process equipment, structural integrity, marine pollution and loss of production. Evidence-based and quantitative risk assessments have therefore identified fire and explosion control as a fundamental component of FPSO design and operation [1,2].

The prevention and mitigation of offshore fires rely on a combination of passive fire protection, detection, emergency shutdown, depressurisation and active firefighting systems. The applicable offshore and marine safety frameworks require firefighting arrangements capable of remaining operational under credible emergency conditions [3–8]. Among these arrangements, the firewater distribution system supplies seawater to deluge systems, fire monitors, hydrants and other fixed firefighting consumers. Its hydraulic performance is directly related to the ability of the installation to cool exposed equipment, limit fire escalation and maintain safe conditions during emergency response [3,6–8].

An offshore firewater system generally comprises diesel-driven main fire pumps, jockey pumps, ring-main pipelines, isolation valves, check valves, pressure safety devices and multiple firefighting consumers distributed across different elevations. Under standby conditions, the network remains pressurised but carries little or no flow. Following fire detection, one or more main pumps may start while deluge valves, hydrants or monitors are activated. These operations produce rapid variations in flow velocity and pressure that cannot be assessed adequately using steady-state calculations alone [9–13].

Hydraulic transients occur whenever the momentum of a moving fluid changes over a sufficiently short period. Pump start-up or shutdown, rapid valve opening or closure, check-valve operation and sudden variations in system demand generate pressure waves that propagate through the network at a velocity governed by the compressibility of the fluid and the elastic response of the pipe wall [9–13]. Depending on the operating sequence and network configuration, water hammer may produce excessive positive pressure, subatmospheric pressure, cavitation, liquid-column separation, pipe vibration, leakage and excessive loading of valves, supports and connected equipment [13–17].

The classical Joukowsky relationship shows that the pressure variation associated with a rapid velocity change depends on the fluid density, wave-propagation velocity and magnitude of the velocity variation [9,10,13]. However, the response of an industrial piping network cannot be described solely using this relationship. Pipe-wall elasticity, unsteady friction, material behaviour, trapped air, network topology, boundary conditions and wave reflections at fittings and branches can substantially modify the attenuation, shape and timing of the pressure waves [14–20]. Consequently, the maximum or minimum pressure may occur far from the component that initiates the transient event.

Negative-pressure transients require particular attention because a local pressure reduction below the vapour pressure of the liquid can produce vapour cavities and separation of the liquid column. The subsequent collapse of these cavities may generate secondary pressure peaks that are more severe than the initial pressure variation [14–16,21]. Experimental investigations have shown that initial flow rate, valve-closing speed and the spatial distribution of cavities strongly influence both cavity length and collapse-induced pressure peaks [21]. Verification of the maximum pressure alone is therefore insufficient; the complete transient pressure envelope must include both upper and lower pressure limits.

The hydraulic response is also strongly influenced by the operating law of the initiating valve. Transient severity depends not only on the total interrupted flow but also on the valve-closing time and the nonlinear relationship between valve position and effective flow area [22,23]. The interaction between the closing time and the characteristic travel time of the pressure wave determines whether the manoeuvre behaves as a rapid or gradual closure. A relatively low-flow consumer operating with a short closing time may consequently produce a more severe transient event than a higher-capacity consumer closing more slowly.

Analytical expressions provide useful preliminary estimates for simple pipelines, but complex branched networks require numerical solution of the one-dimensional continuity and momentum equations [9–13,24]. The Method of Characteristics (MOC) remains one of the most established numerical approaches because it transforms the governing partial

differential equations into ordinary differential equations along characteristic wave trajectories [9,10,13,24]. This formulation provides an efficient means of representing wave propagation and reflection in networks containing pumps, valves, branches and multiple hydraulic boundary conditions.

The accuracy of a conventional one-dimensional model nevertheless depends on the physical mechanisms included in the formulation. Frequency-dependent friction, viscoelastic pipe-wall behaviour, fluid–structure interaction, trapped air and distributed or discrete cavitation may significantly alter the calculated pressure response [14–20]. Failure to represent these mechanisms can lead to differences between calculated and measured attenuation rates, wave shapes and arrival times.

Higher-dimensional computational fluid dynamics models can provide detailed information about local flow structures, turbulence and component-scale behaviour during rapid valve operations. However, their computational cost remains considerably greater than that of one-dimensional approaches, particularly for complete industrial piping networks [24,25]. For large offshore systems, one-dimensional transient modelling therefore provides an appropriate engineering compromise between physical fidelity, computational efficiency and the ability to represent the complete network.

Several strategies can be adopted to mitigate unacceptable hydraulic transients. These include modifying pump-control sequences and valve-operating laws, installing surge vessels or hydropneumatic tanks, using air or pressure-relief valves, selecting appropriate check-valve characteristics and modifying the location of protective components [9–12,23,26]. The effectiveness of each solution depends on the initiating event and its interaction with the entire hydraulic network. A measure that attenuates positive pressure close to the pump may not necessarily prevent underpressure or cavitation in a remote branch.

Despite the extensive literature on hydraulic transients, most published studies address water-transmission pipelines, pumping stations or comparatively simple networks. Applications to complete offshore piping networks remain limited. Sotoodeh [23] examined water hammer associated with check-valve operation in the offshore industry and discussed the influence of valve selection and dynamic behaviour. Park et al. [27] investigated a seawater-treatment system installed on an offshore floating production unit and demonstrated that valve characteristics and closing time have a decisive influence on the calculated pressure response.

However, limited information is available regarding the transient behaviour of FPSO firewater ring mains subjected to multiple representative emergency operating sequences. Previous studies have rarely compared pump-driven and valve-driven transients within the same offshore firewater network. The governing case cannot necessarily be inferred from the nominal flow rate of the affected consumer because transient severity also depends on operating time, wave travel, component location and interactions within the ring main.

Furthermore, few published studies have quantified the combined effect of check-valve relocation and pressure safety valve set-point modification on both maximum and minimum pressures. This limitation is important because an optimisation intended to reduce overpressure may affect the underpressure response elsewhere in the network. A pressure-protection arrangement should therefore be assessed using several representative emergency scenarios and both limits of the transient pressure envelope.

The objective of this study is to evaluate the transient hydraulic response of an FPSO firewater distribution system and to assess the effectiveness of a modified pressure-protection arrangement. A detailed numerical model developed in PIPENET Transient is used to analyse three operating scenarios: simultaneous fire-pump start-up and deluge-

valve opening, deluge-valve closure while the main pump remains operational, and fire-monitor closure while the main pump remains operational.

For each scenario, the original configuration is compared with a modified arrangement in which the check valve is relocated immediately downstream of the fire-pump discharge flange and the Pressure Safety Valve (PSV) set pressure is reduced from 17.5 barg to 16.5 barg. The analysis considers maximum and minimum pressures, pressure-wave propagation, pump response, firefighting-consumer behaviour and system stabilisation.

The principal contributions of this study are: (i) transient assessment of a complete industrial firewater ring main under multiple emergency operating sequences; (ii) direct comparison of the pump-start-up, deluge-valve-closure, and fire-monitor-closure operating cases; (iii) comparative identification of the governing system-level pressure envelopes using both overpressure and underpressure acceptance criteria; and (iv) quantitative evaluation of a practical PSV and check-valve modification as a pressure-surge mitigation strategy.

2. Materials and Methods

2.1. Description of the Firewater Distribution System

The investigated hydraulic network corresponds to the firewater distribution system of an FPSO unit. Its function is to provide seawater to the onboard firefighting installation during emergency operation. As a safety-critical system, the firewater network must supply the required flow rate and pressure to the activated consumers while maintaining hydraulic integrity during rapid operational changes [3,6–8].

Figure 1 presents a simplified layout of the investigated FPSO firewater system. The numerical model was developed using the available engineering documentation, including General Arrangement drawings, Piping and Instrumentation Diagrams and the three-dimensional plant model. The principal characteristics of the system are summarised in Table 1.



Figure 1. Simplified layout of the investigated FPSO Firewater distribution system.

Table 1. Principal characteristics of the investigated firewater system.

Parameter	Specification
Installation type	Floating Production Storage and Offloading unit
Distribution configuration	Closed firewater ring main
Working fluid	Seawater
Main fire pumps	Two diesel-driven centrifugal pumps (one duty and one standby)
Jockey pumps	Two pumps in duty/standby configuration
Firefighting consumers	Deluge systems, fire monitors and hydrants
Pressure protection	Pressure Safety Valve
Numerical representation	One-dimensional transient hydraulic model
Simulation software	PIPENET Vision Transient
Engineering documentation	GA drawings, P&IDs and three-dimensional plant model

The closed ring-main configuration provides alternative flow paths between the fire pumps and firefighting consumers. This arrangement improves hydraulic redundancy and allows individual sections of the network to be isolated for maintenance or following accidental damage without completely interrupting water supply.

Under standby conditions, the network remains pressurised with negligible flow. The jockey pumps compensate for minor leakage and maintain the initial system pressure without requiring operation of the main fire pumps. Following fire detection, the automatic start-up of a main fire pump and activation of one or more firefighting consumers generate rapid changes in flow velocity and pressure. The resulting response may include pressure surges, oscillations and local underpressure, requiring analysis under transient rather than exclusively steady-state conditions [9–13].

2.2. Numerical Model

A one-dimensional hydraulic model of the complete firewater distribution network was developed using PIPENET Vision Transient Module, Version 1.12.0.4255 (Sunrise Systems Limited, Cambridge, UK).

The physical firewater system includes two diesel-driven main fire pumps arranged in a duty/standby configuration. For the transient scenarios analysed in this study, the duty pump (Fire Pump A) was considered as the operating main fire pump, while the second pump remained in standby condition. Therefore, only one main fire pump is represented as active in the investigated transient model.

The hydraulic network was discretised into interconnected pipe sections and nodes. Each pipe section was defined using its internal diameter, length, elevation, material properties and hydraulic roughness. Local pressure losses associated with fittings and inline equipment were represented using the corresponding loss coefficients. Pumps, operating valves, check valves, pressure safety devices and firefighting consumers were implemented as individual hydraulic components. A simplified representation of the complete PIPENET transient model is presented in Figure 2.

The resulting model comprises 128 network components/elements and 112 hydraulic and information nodes, including:

- Seventeen specifications
- Ninety-four pipe sections;
- Seven operating valves;
- One non-return valve;
- One pressure safety valve;
- Two vacuum breakers;
- One main fire pump;

- Two general pressure-loss components;
- One analogue sensor;
- One transfer function; and
- One ON/OFF switch.

The working fluid was defined as seawater at an operating temperature of 30 °C. The initial steady-state solution was calculated before each transient simulation to establish consistent pressure and flow conditions throughout the network.

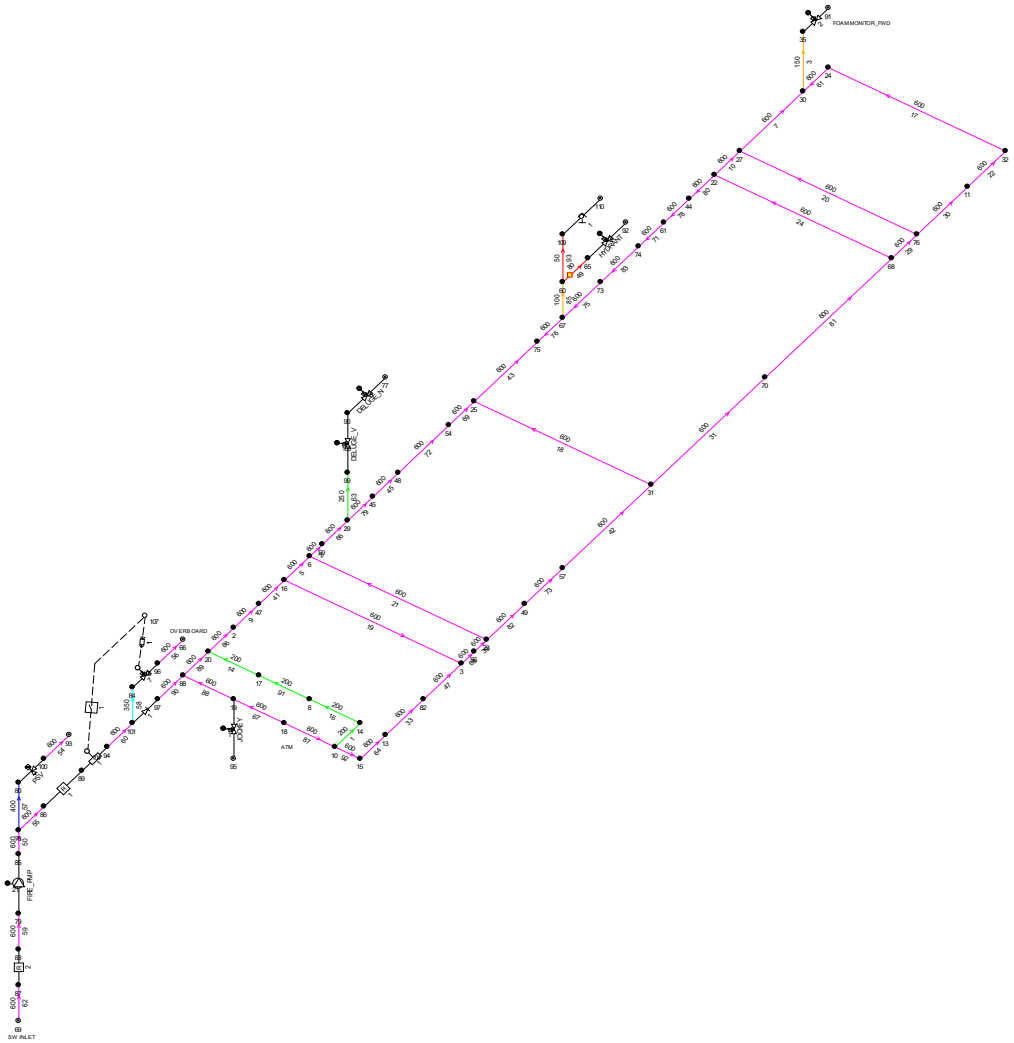

Figure 2. Simplified representation of the PIPENET transient model showing Fire Pump A, the firewater ring main, pressure-protection devices, and principal firefighting consumers.

The transient calculations were based on the one-dimensional continuity and momentum equations solved using the Method of Characteristics. This method is widely used for industrial hydraulic networks because it provides an efficient representation of pressure-wave propagation and reflection while allowing the inclusion of complex boundary conditions associated with pumps, valves and branched piping systems [9,10,13,24].

The numerical model assumes one-dimensional compressible flow and elastic pipe-wall behaviour. The model does not explicitly resolve local three-dimensional flow structures or the dynamic structural response of the piping system. These assumptions are consistent with standard engineering practice for system-level transient analysis but should be considered when interpreting pressure-wave attenuation and local component loading [15–20,24,25].

2.3. Model Input Data

The accuracy of a transient hydraulic analysis depends on the consistent definition of the fluid properties, pipe characteristics, pump operating data, component loss coefficients and system boundary conditions. The input data used in the present model were extracted from the engineering documentation of the investigated FPSO, including GA drawings, P&IDs, the three-dimensional plant model, equipment data sheets and pump performance curves. The main fire pumps were supplied by Sulzer Ltd (Winterthur, Switzerland), the operating valves were supplied by Mil Inbal Valves Ltd. (Rishon LeZion, Israel), and the pressure safety valve (PSV) was supplied by LESER GmbH & Co. KG (Hamburg, Germany).

The firewater system uses seawater at an operating temperature of 30 °C. The seawater properties adopted in the numerical model were defined based on the engineering design data and project-specific input information used for the development of the investigated FPSO firewater model. The adopted density was 1021.769 kg/m^3, the dynamic viscosity was 0.861 cP, and the bulk modulus was 2.20 GPa. The vapour pressure used as the minimum allowable pressure was −0.971 barg. Since seawater properties depend on temperature, salinity and pressure, the adopted values should be regarded as design-specific model inputs rather than universally applicable seawater properties. Pressure values below the adopted vapour-pressure limit were considered indicative of potential vapour-cavity formation and liquid-column separation, consistent with established transient-flow theory [13,14,21].

The physical firewater installation includes both Copper Alloy and RTRP/GRE piping, as identified in the FPSO engineering documentation. Copper Alloy is present in the dry sections, whereas RTRP/GRE is used in the wet sections continuously exposed to seawater. For the transient numerical calculations, however, the pipe-wall mechanical properties were represented using the RTRP/GRE composite material properties. Therefore, the material information reported in Table 2 distinguishes between the materials present in the physical installation and the material properties adopted in the transient model. The principal fluid, pipe and pump parameters adopted in the model are summarised in Table 2.

Table 2. Input parameters adopted in the transient hydraulic model.

Category	Parameter	Value
Working fluid	Fluid	Seawater
	Operating temperature	30 °C
	Density	1021.769 kg/m^3
	Dynamic viscosity	0.861 cP
	Bulk modulus	2.20 GPa
	Vapour pressure	−0.971 barg
Pipe material Pipe material	Dry section	Copper Alloy
	Wet section	RTRP/GRE
	Nominal pipe design pressure	18 barg
	Young's modulus (RTRP/GRE)	18.365 GPa
	Poisson's ratio (RTRP/GRE)	0.58
	Absolute roughness	0.01 mm
	Hazen–Williams coefficient	150
Main fire pump	Rated capacity	2830 m^3/h
	Rated discharge pressure	15 barg
	Design pressure	18 barg

Table 2. *Cont.*

Category	Parameter	Value
Pressure criteria	Maximum allowable pressure below Main Deck	17.5 barg
	Maximum allowable pressure above Main Deck	15.5 barg
	Minimum allowable pressure	−0.971 barg
Simulation	Initial ring-main pressure	9 barg
	Total simulation time	60 s

The pressure limits adopted in the analysis distinguish between piping located above and below the Main Deck because these sections are subject to different design requirements. Compliance was assessed by comparing the maximum and minimum pressure envelopes calculated throughout the network with the corresponding allowable limits.

The hydraulic representation of the firefighting consumers was parameterised using the design/reference flow-rate and pressure pairs listed in Table 3. The corresponding metric valve flow coefficients, K_v, $\boldsymbol{K_v}$ were introduced into PIPENET to reproduce the hydraulic characteristics of each component. Consequently, the instantaneous flow rate during a transient simulation depends on the local pressure conditions and is not constrained to remain equal to the tabulated design flow rate.

Table 3. Hydraulic characteristics of the principal valves and firefighting consumers.

Component	Design Flow Rate (m^3/h)	Reference Pressure (Barg)	Flow Coefficient, K_v ($m^3\ h^{-1}\ bar^{-1/2}$)
Pressure Safety Valve	1700	17.5	406.378
Overboard valve	1700	17.5	406.378
Jockey pump	75	11.0	22.613
Deluge valve	880	7.0	332.609
Virtual deluge-network valve	880	7.0	332.609
Hydrant 1	30	7.0	11.339
Hydrant 2	30	7.0	11.339
Fire monitor	120	7.0	45.356

The deluge system was represented by two valves connected in series. The first component reproduces the operating characteristics of the physical deluge valve, including its time-dependent opening or closing sequence. The second is a virtual hydraulic component used to reproduce the required pressure and flow conditions of the downstream deluge network. This approach enables the demand of the protected area to be represented without modelling every individual spray nozzle.

The main fire pump was represented in PIPENET using its characteristic performance curve, with a rated capacity of 2830 m^3/h and a rated discharge pressure of 15 barg, as specified in Table 2. Its operating point was therefore determined dynamically by the instantaneous hydraulic resistance of the network. The jockey pump was represented by an equivalent pressure boundary condition rather than by an explicit pump performance curve. During the initial standby condition, this boundary maintained the firewater ring main at 9 barg. In Case I, after establishment of Main Fire Pump A operation, the jockey-pump boundary was transitioned to the closed state over a period of 0.5 s according to the prescribed operating sequence. In Cases II and III, the jockey-pump boundary was excluded because the main fire pump was already operating at the beginning of the simulation.

All simulations were conducted over a total duration of 60 s. This simulation period was selected to capture the relevant transient response associated with the investigated

operating events, including the initial pressure-wave generation, subsequent wave propagation and reflections throughout the ring main, and the attenuation of the dominant pressure and flow oscillations after completion of the pump or valve operation. The 60 s duration also provided a sufficiently long post-event interval to assess whether the hydraulic variables approached a stabilised operating regime. The component-operating schedules for the three transient scenarios are described in the following subsection

2.4. Simulation Scenarios

Three transient operating scenarios were analysed to evaluate the response of the FPSO firewater system to representative emergency operations. The selected cases include both flow acceleration and flow interruption events generated by pump and valve operations. The same network geometry, fluid properties and pipe characteristics were used in all simulations, while the initial component states and operating sequences were varied.

Each scenario was simulated for both the original and modified pressure-protection configurations. In the original configuration, the PSV set pressure was 17.5 barg. In the modified configuration, the check valve was relocated immediately downstream of the main fire-pump discharge flange and upstream of the PSV, while the PSV set pressure was reduced to 16.5 barg. All other parameters were maintained unchanged to allow direct comparison. The three operating sequences are illustrated in Figure 3 and summarised in Table 4.

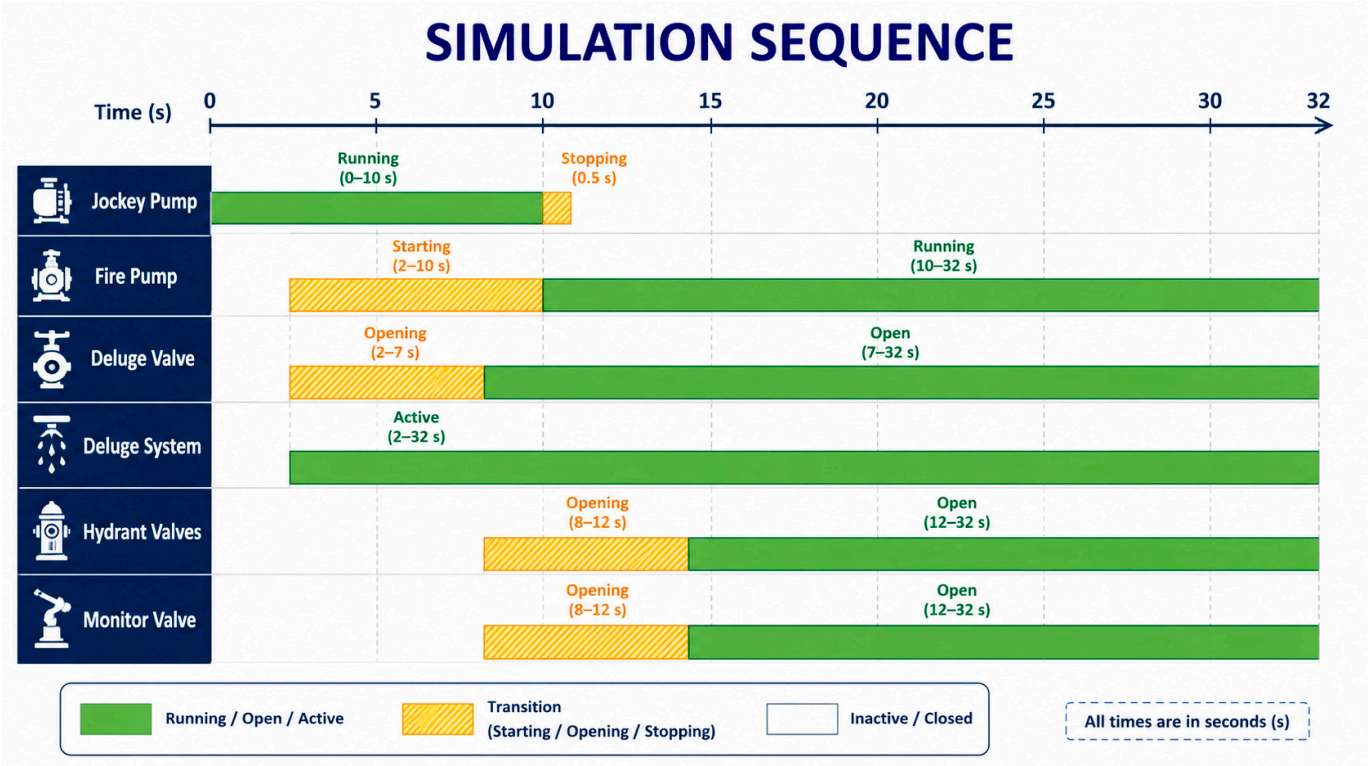

(**a**)

Figure 3. *Cont.*

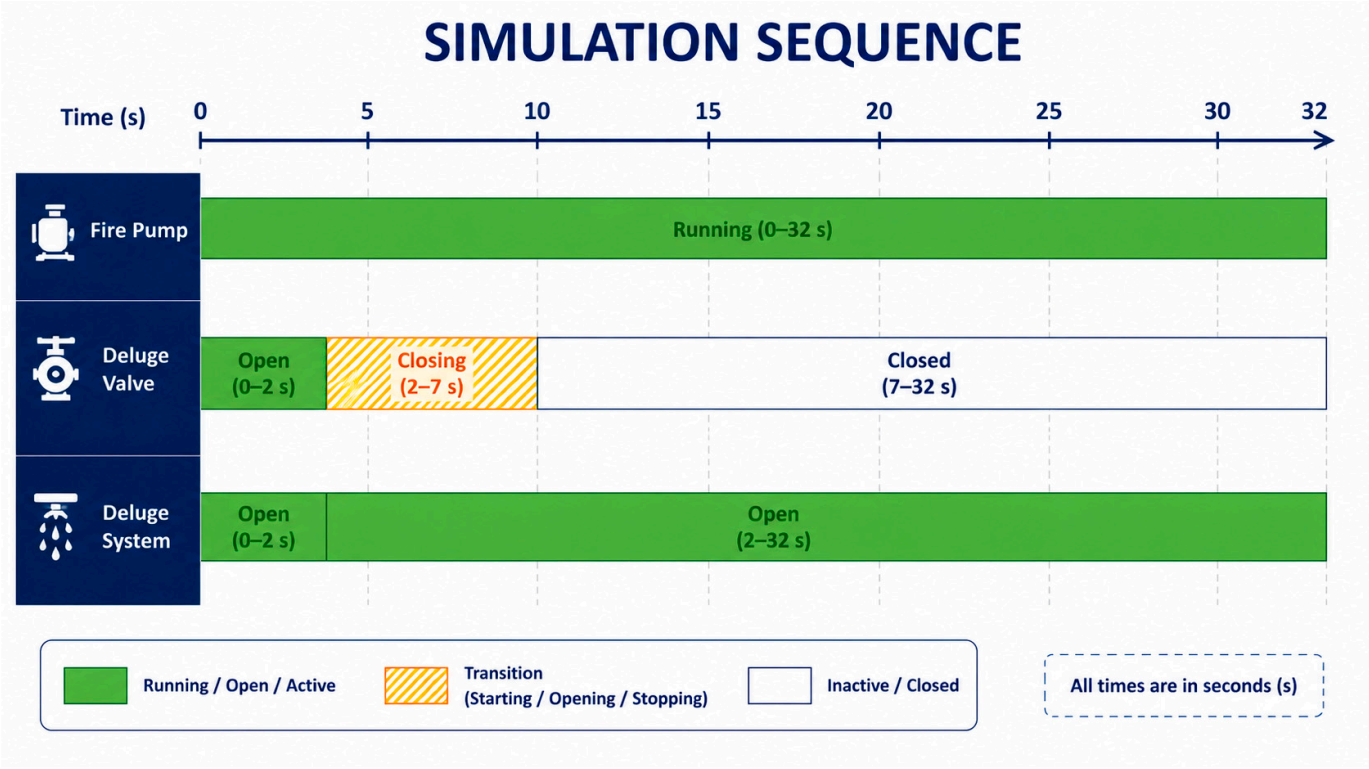

(**b**)

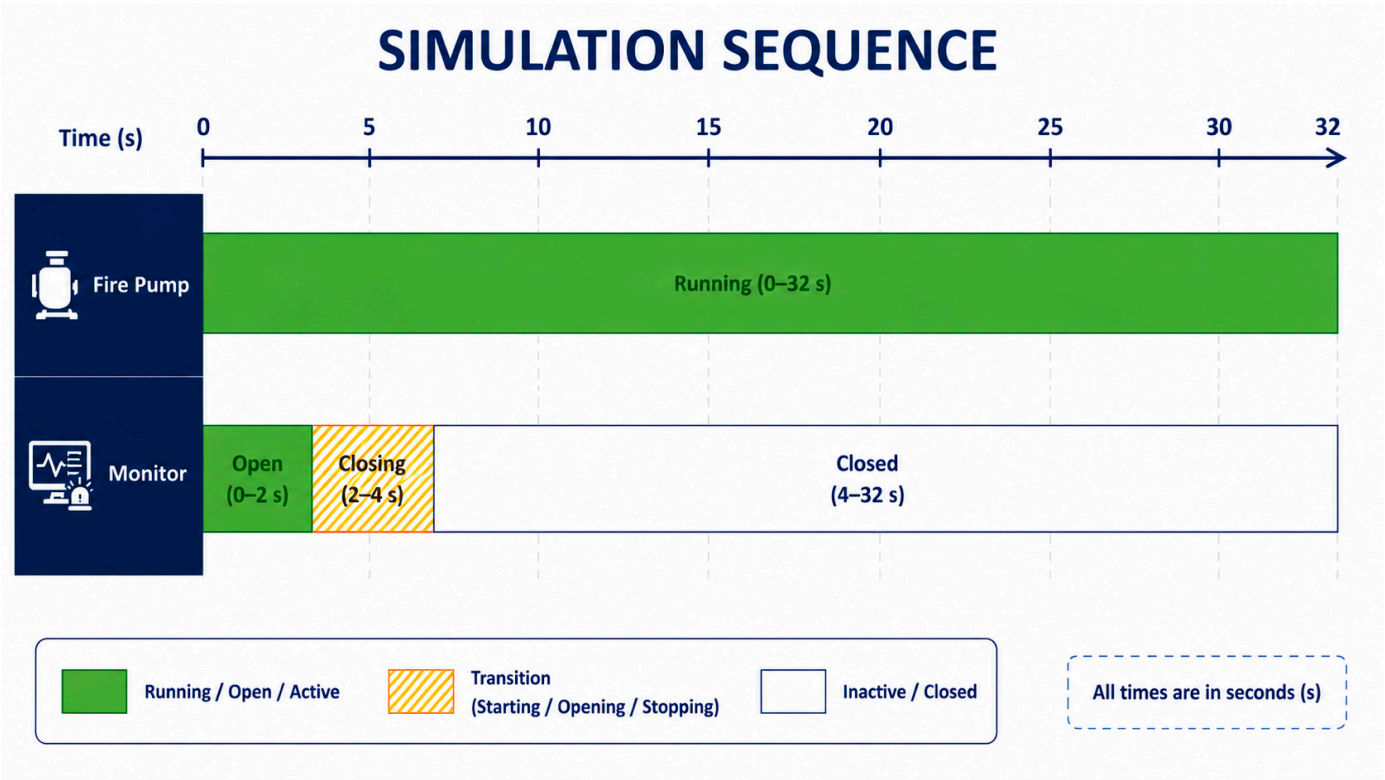

(**c**)

Figure 3. Operating sequences adopted for the transient simulations: (**a**) Case I—deluge valve opening and main fire-pump start-up; (**b**) Case II—deluge valve closure during continuous pump operation; (**c**) Case III—fire-monitor closure during continuous pump operation. The operating-sequence diagrams are shown up to 32 s for clarity; the component states remain unchanged thereafter until the end of the 60 s simulation.

Table 4. Operating sequences adopted for the transient simulations.

Case	Hydraulic Event	Initial Condition	Component Operation	Primary Assessment Objective
I	Deluge valve opening and main fire-pump start-up	Ring main maintained at 9 barg by the jockey pump	Deluge valve opens from 2 to 7 s; Fire Pump A starts from 2 to 10 s; hydrants and monitor open from 8 to 12 s	Evaluation of the pressure transients generated during emergency system activation
II	Deluge valve closure with Fire Pump A operating	Main pump operating and deluge valve fully open	Deluge valve closes from 2 to 7 s; main pump remains operational	Evaluation of overpressure generated by progressive interruption of the deluge-system flow
III	Fire-monitor closure with Fire Pump A operating	Main pump operating and fire monitor fully open	Fire monitor closes from 2 to 4 s; main pump remains operational.	Evaluation of local and system-level pressure response during the fire-monitor operating sequence

2.4.1. Case I—Deluge Valve Opening and Main Fire-Pump Start-Up

Case I represents the emergency activation of the firewater system from its pressurised standby condition. At the beginning of the simulation, the ring main is maintained at 9 barg by the jockey pump, while the main fire pump and firefighting consumers are inactive.

The deluge valve begins to open at t = 2 s and reaches its fully open position at t = 7 s. The reduction in ring-main pressure initiates the start-up of Fire Pump A at t = 2 s. The pump reaches its operating condition at t = 10 s, corresponding to a start-up duration of 8 s.

The hydrants and fire monitor begin opening at t = 8 s and reach their fully open positions at t = 12 s. After confirmation that the main fire pump is operating, the equivalent jockey-pump pressure boundary is transitioned to the closed state over 0.5 s. The virtual valve representing the downstream deluge network changes progressively during the filling and activation period to reproduce the gradual establishment of the spray-system demand.

This scenario combines rapid flow acceleration, pump start-up and activation of several firefighting consumers. It was used to determine the maximum and minimum pressures produced during emergency system activation and the time required for the pump and consumer branches to reach stable hydraulic conditions.

2.4.2. Case II—Deluge Valve Closure with the Main Pump Operating

Case II considers closure of the deluge valve while Fire Pump A remains in continuous operation. At the beginning of the simulation, the deluge valve is fully open, and the fire pump supplies the corresponding demand. The jockey pump is excluded because the main fire pump provides the system pressurisation.

The physical deluge valve begins to close at t = 2 s and reaches its fully closed position at t = 7 s, corresponding to a closing duration of 5 s. The main pump remains operational throughout the simulation. The hydrants and fire monitor remain closed, ensuring that the calculated transient is generated exclusively by the reduction in flow through the deluge branch.

This operating sequence isolates the transient response produced by progressive flow deceleration. It was used to evaluate the conversion of fluid kinetic energy into pressure energy, the displacement of the pump operating point and the maximum pressure developed above and below the Main Deck.

2.4.3. Case III—Fire-Monitor Closure with the Main Pump Operating

Case III investigates closure of the fire monitor while Fire Pump A remains in continuous operation. Initially, the monitor is fully open, while the deluge system and the two hydrants remain closed. The jockey pump is excluded from the model.

The fire monitor remains fully open until t = 2 s and closes between t = 2 s and t = 4 s, corresponding to a closing duration of 2 s and reducing the branch flow to zero. Although the nominal monitor flow is substantially lower than the deluge-system flow, the short closing time produces a rapid local change in velocity and generates pressure waves that propagate throughout the ring main.

This scenario was selected to evaluate the system response associated with the rapid interruption of a relatively small local demand and to compare it with the responses obtained for the other investigated operating sequences. Both maximum and minimum pressures were assessed over the complete simulation interval in order to characterise the resulting system-level pressure envelope.

2.5. Governing Equations

Transient flow in pressurised piping systems is governed by the one-dimensional equations of mass and momentum conservation. Under the assumptions of compressible unsteady flow in an elastic pipe, pressure-wave propagation results from the interaction between fluid compressibility and pipe-wall deformation [9,10,13].

The continuity equation is expressed as:

$$\frac{\partial H}{\partial t} + \frac{a^2}{gA}\frac{\partial Q}{\partial x} = 0, \tag{1}$$

The momentum equation is written as:

$$\frac{1}{gA}\frac{\partial Q}{\partial t} + \frac{\partial H}{\partial x} + \frac{fQ|Q|}{2gDA^2} = 0, \tag{2}$$

Equations (1) and (2) are presented in their conventional one-dimensional form to describe the theoretical basis of transient-flow analysis. The friction term shown in Equation (2) should be distinguished from the friction-loss formulation implemented in the present PIPENET model, for which the Hazen–Williams formulation was used.

For a rapid variation in flow velocity, the corresponding pressure change can be estimated using the Joukowsky equation:

$$\Delta P = \rho a \Delta V, \tag{3}$$

Equation (3) provides a preliminary estimate of the pressure variation generated by a rapid valve operation or pump transient. Its direct application assumes an effectively instantaneous velocity change and does not account for the multiple wave reflections, branched flow paths and time-dependent component characteristics present in the investigated firewater network [9,13].

The governing equations were solved using the Method of Characteristics implemented in PIPENET Vision Transient. The MOC transforms the coupled partial differential equations into compatibility equations along characteristic wave trajectories. This enables pressure and flow variations to be calculated throughout networks containing pipes, pumps, valves, branches and hydraulic boundary conditions [9,10,13,24].

The one-dimensional continuity and momentum equations provide the theoretical basis for the transient-flow formulation. In the numerical model used in the present study, frictional pressure losses were calculated using the Hazen–Williams formulation, with a

Hazen–Williams coefficient of 150 as specified in Table 2. The Darcy–Weisbach formulation was not used for the friction-loss calculations in the present PIPENET simulations. Local losses associated with fittings were represented according to the NFPA 2013 rules available in PIPENET. The same friction-loss representation was applied consistently to the initial hydraulic condition and the subsequent transient analyses. Frequency-dependent friction, fluid–structure interaction, viscoelastic pipe-wall behaviour and detailed three-dimensional flow structures can influence pressure-wave attenuation and timing but were not explicitly resolved in the present model [15–20,24,25]. These limitations are considered when interpreting the calculated pressure extrema and stabilisation behaviour.

2.6. Numerical Procedure and Assessment Criteria

Each transient calculation was preceded by a steady-state solution used to establish the initial pressure and flow conditions throughout the firewater network. The model input was subsequently checked using the internal PIPENET consistency and error-checking procedure. The final model contained 128 network components/elements and 112 nodes, including information nodes, and was processed without input errors or warnings.

The transient simulations were performed using the program-determined fixed time step (FTS) of 0.4760×10^{-3} s. Numerical convergence was assessed using the absolute and relative convergence tolerances defined in the PIPENET calculation settings. The exact numerical tolerance values were not available in the archived simulation records and are therefore not reported.

For the purposes of this study, the stabilisation time was defined as the earliest time after completion of the initiating pump or valve operation at which the monitored pressure and flow-rate histories entered and remained within $\pm 5\%$ of their final quasi-steady values for the remainder of the analysed simulation interval. This criterion was applied consistently to the original and modified configurations when comparing the duration of the transient response.

The same network geometry, pipe properties, fluid characteristics, pump curve and consumer data were used for all simulations. For each operating scenario, two calculations were performed:

- the original configuration, with the existing check-valve position and a PSV set pressure of 17.5 barg;
- the modified configuration, with the check valve relocated immediately downstream of the main fire-pump discharge flange and the PSV set pressure reduced to 16.5 barg.

This paired simulation approach isolates the influence of the proposed protection modification because all other model parameters and operating sequences remain unchanged.

The hydraulic response was evaluated using the following indicators:

- minimum pressure within the complete network;
- maximum pressure above the Main Deck;
- maximum pressure below the Main Deck;
- fire-pump suction and discharge pressures;
- fire-pump discharge flow rate;
- pressure and flow-rate histories at the deluge valve;
- pressure response at the hydrant branches;
- pressure and flow-rate histories at the fire monitor;
- amplitude and persistence of pressure oscillations; and
- time required to reach a stabilised hydraulic regime.

The calculated maximum pressures were compared with the adopted allowable limits of 15.5 barg above the Main Deck and 17.5 barg below the Main Deck. Pressures below the adopted minimum allowable pressure of -0.971 barg were interpreted as an indication

of potential transient cavitation within the limitations of the single-phase model, rather than as a direct prediction of vapour-cavity dynamics. A scenario was considered hydraulically acceptable when the complete pressure envelope remained within these upper and lower limits.

The relative change produced by the modified configuration was calculated as:

$$R = \frac{X_{mod} - X_{orig}}{X_{orig}} \times 100, \quad (4)$$

where X_{orig} and X_{mod} denote the values obtained for the original and modified configurations, respectively. For maximum pressure and pressure-oscillation amplitude, a negative value of R indicates a reduction. For minimum pressure, an increase indicates an improved margin against vapour formation.

Because full-scale measurements were not available, the present analysis constitutes a comparative numerical assessment rather than an experimentally validated prediction. Model credibility was supported through consistency with the engineering documentation, use of established one-dimensional transient-flow equations and application of identical assumptions to the original and modified configurations. The results should therefore be interpreted primarily in terms of relative pressure reduction, identification of critical scenarios and compliance with the adopted design limits.

3. Results and Discussion

3.1. Transient Hydraulic Response During Case I

The transient response of the diesel-driven fire pump was evaluated for the emergency operating sequence involving the simultaneous start-up of the main fire pump and the opening of the deluge valve. The evolution of the pump operating parameters is presented in Figure 4, where the variations in the suction pressure, discharge pressure and discharge flow rate are plotted as a function of time.

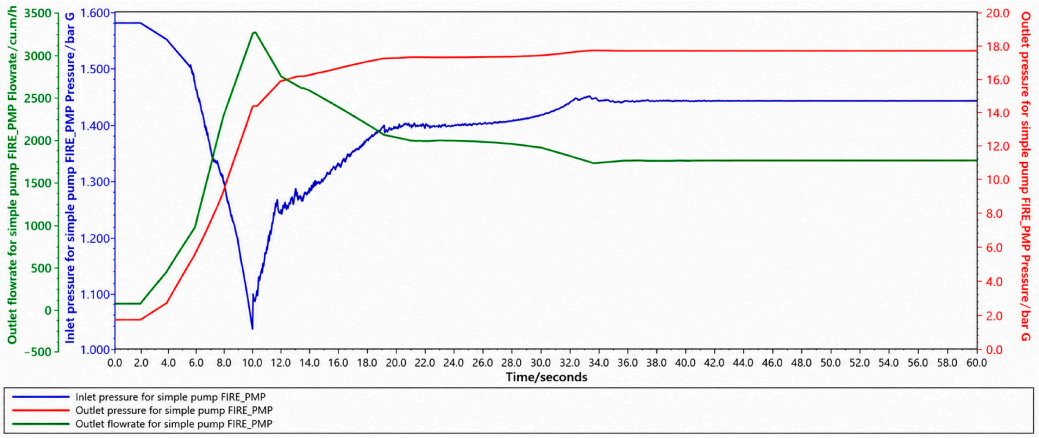

Figure 4. Transient response of the fire pump during Case I (simultaneous opening of the deluge valve and start-up of the main fire pump).

Immediately after the start-up sequence, the pump experienced a rapid transition from the initial operating condition to the required firefighting duty point. During this period, both the pressure and flow rate varied significantly as the hydraulic network adjusted to the sudden increase in water demand. The most pronounced changes occurred during the first seconds of the transient event, after which the hydraulic parameters progressively approached stable operating conditions.

The results indicate that the discharge pressure increased continuously as the pump established the required head for supplying the firewater distribution network, while the discharge flow rate rapidly reached the value required by the activated consumers. At the same time, the suction pressure exhibited a temporary reduction associated with the rapid acceleration of the water column and the transient redistribution of pressure within the system. After the initial transient period, the recorded variables gradually stabilised, indicating that the hydraulic system reached a new equilibrium corresponding to the emergency operating condition.

Within Case I, the most pronounced variations in the pump operating parameters occur during the start-up phase, highlighting the importance of transient analysis when assessing emergency system activation.

The transient response of the deluge valve was analysed to evaluate the hydraulic behaviour of the firewater distribution network during emergency activation. As shown in Figure 5, the simulation records the evolution of the inlet pressure, outlet pressure, inlet flow rate and valve opening throughout the transient event. These parameters provide a comprehensive representation of the interaction between valve actuation and the hydraulic response of the network.

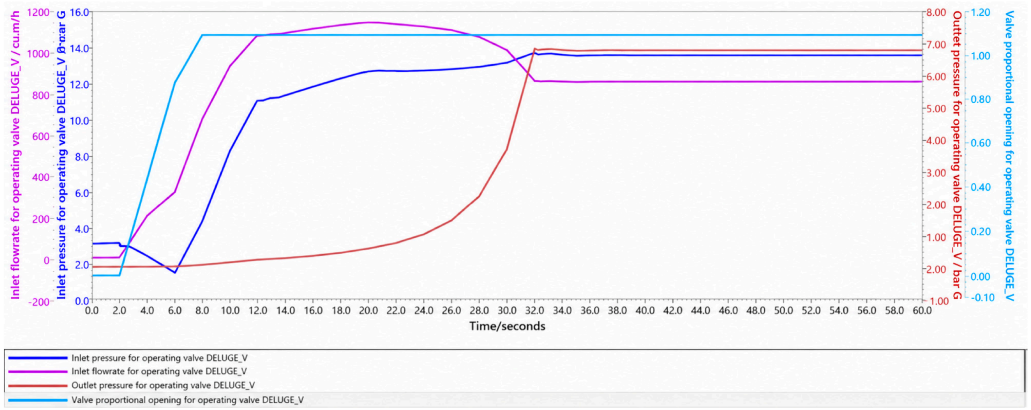

Figure 5. Transient response of the deluge valve during Case I (simultaneous opening of the deluge valve and start-up of the main fire pump).

At the beginning of the transient event, the deluge valve opens progressively according to the predefined operating sequence, resulting in a rapid increase in the flow supplied to the protected area. The increase in valve opening is accompanied by a corresponding rise in the inlet flow rate, while the inlet and outlet pressures undergo significant variations before gradually approaching stable operating conditions. This behaviour reflects the redistribution of hydraulic energy within the firewater network immediately after the emergency demand is initiated.

Once the valve reaches its fully open position, the hydraulic variables progressively stabilise, indicating that the interaction between the diesel-driven fire pump and the distribution network is sufficient to establish a new steady operating regime. Although transient pressure fluctuations are observed during the opening sequence, no sustained oscillatory behaviour develops after the valve reaches its final position, demonstrating the ability of the system to accommodate the sudden increase in water demand.

The obtained results indicate that the valve opening sequence governs the initial transient response of the downstream branch and therefore represents one of the critical phases to be considered during the hydraulic design of offshore firewater systems. Proper coordination between pump start-up and valve actuation contributes to limiting transient pressure fluctuations and ensuring stable operation under emergency conditions.

The transient hydraulic response of the hydrant branch during the emergency activation sequence is presented in Figure 6.

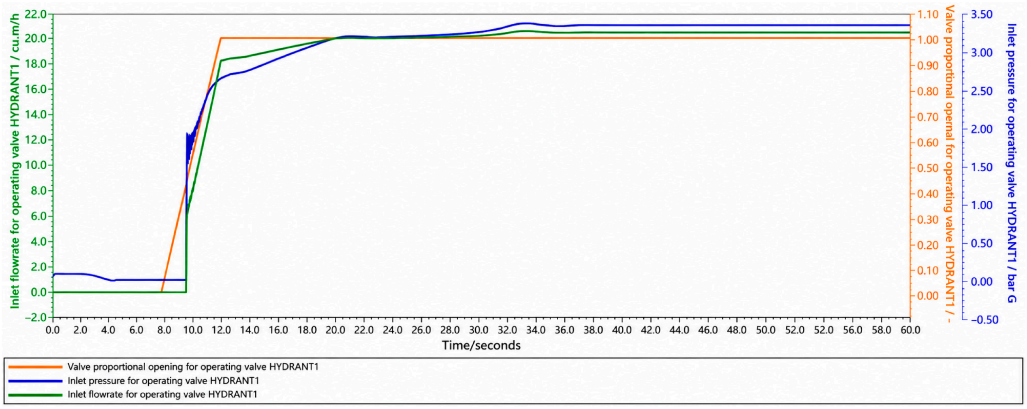

Figure 6. Transient response of the hydrant branch during Case I (simultaneous opening of the deluge valve and start-up of the main fire pump).

Following the initiation of the emergency sequence, the hydrant valve opens according to the predefined operating schedule, producing a rapid increase in the supplied flow rate. The pressure response follows the establishment of the flow conditions, with a short transient period before reaching a stable operating regime. The close correlation between valve opening, flow development and pressure evolution indicates that the hydrant branch responds rapidly to the changing hydraulic conditions imposed by the firewater network.

After the initial transient, both the inlet pressure and flow rate remain practically constant, demonstrating that the branch operates under stable hydraulic conditions once the emergency demand has been fully established. No significant pressure oscillations are observed after the stabilisation period, indicating that the transient generated by the simultaneous pump start-up and deluge valve opening is effectively damped before affecting the long-term operation of the hydrant branch.

These results confirm that the analysed hydrant branch maintains stable hydraulic performance during emergency activation and that the transient effects are limited to the initial operating period. Consequently, the branch reaches a stable hydraulic operating condition without evidence of persistent hydraulic instability.

To reduce the pressure peaks generated during the emergency activation sequence, a modified pressure protection arrangement was subsequently investigated. The check valve was relocated immediately downstream of the main fire pump discharge flange and upstream of the pressure safety valve. In addition, the PSV set pressure was reduced from 17.5 barg to 16.5 barg, enabling earlier activation under transient overpressure conditions. All other model parameters, boundary conditions and operating sequences were maintained unchanged to ensure direct comparison with the original configuration. The transient response of the fire pump obtained for the modified configuration is presented in Figure 7.

As shown in Figure 7, the modified configuration produces a more stable transient response at the pump discharge. The minimum suction pressure decreases slightly from approximately 1.04 barg to 1.00 barg, while the stabilised suction pressure decreases from approximately 1.45 barg to 1.35 barg. The steady-state discharge pressure is only marginally affected, decreasing from approximately 17.5 barg to approximately 16.9 barg. Therefore, the modification does not significantly alter the final pump operating point.

A more pronounced improvement is observed in the duration and amplitude of the transient response. The pump stabilisation time decreases from approximately 35 s in

the original configuration to approximately 20 s after modification, corresponding to a reduction of approximately 42.9%. At the same time, the pressure oscillations occurring during pump acceleration are visibly attenuated. The peak discharge flow rate remains close to 3200 m^3/h, indicating that the modified arrangement does not restrict the pump response during emergency activation. Overall, the modification reduces the severity and duration of the transient event while preserving the required hydraulic operation of the firewater system. The response of the deluge valve under the modified pressure-protection arrangement is shown in Figure 8.

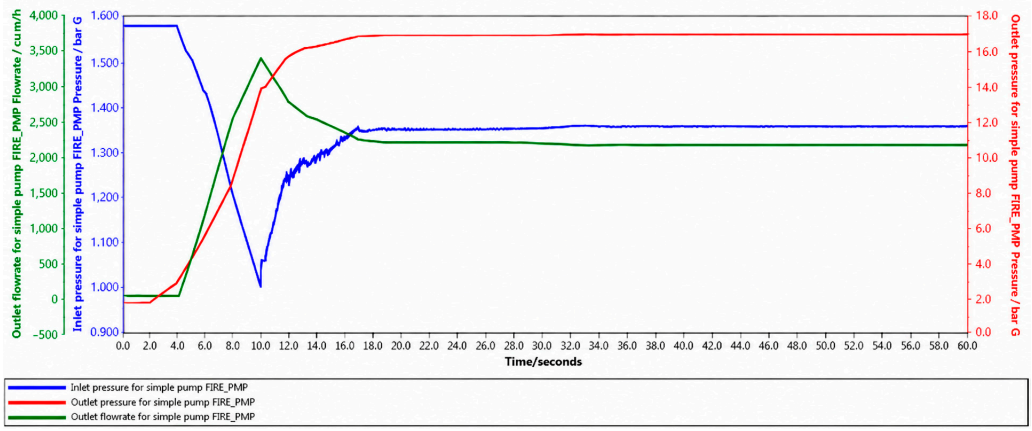

Figure 7. Transient response of the fire pump during Case I for the modified PSV arrangement.

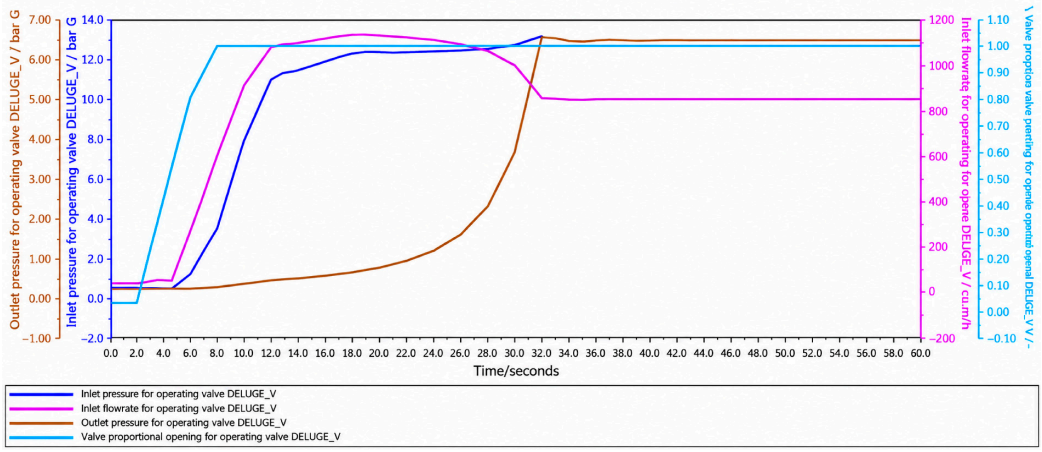

Figure 8. Transient response of the deluge valve during Case I for the modified PSV arrangement.

The valve-opening sequence remains unchanged, with the deluge valve beginning to open at t = 2 s and reaching its fully open position at approximately t = 7 s. The transient flow rate reaches approximately 1100 m^3/h before stabilising at approximately 800 m^3/h in both configurations. Consequently, relocating the check valve and reducing the PSV set pressure do not adversely affect the water supply delivered to the deluge system.

Only limited differences are observed in the pressure response at the deluge valve. The minimum inlet pressure decreases from approximately 1.60 barg to 1.55 barg, corresponding to a variation of approximately 3.1%, whereas the stabilised inlet pressure decreases from approximately 13.95 barg to 13.60 barg. However, the stabilisation time is reduced from approximately 35 s to 33 s, representing an improvement of approximately 5.7%. These results demonstrate that the proposed modification primarily influences the pressure-wave propagation near the pump discharge while preserving the hydraulic performance of the deluge branch. Figure 9 presents the transient response of the hydrant branch for the modified configuration.

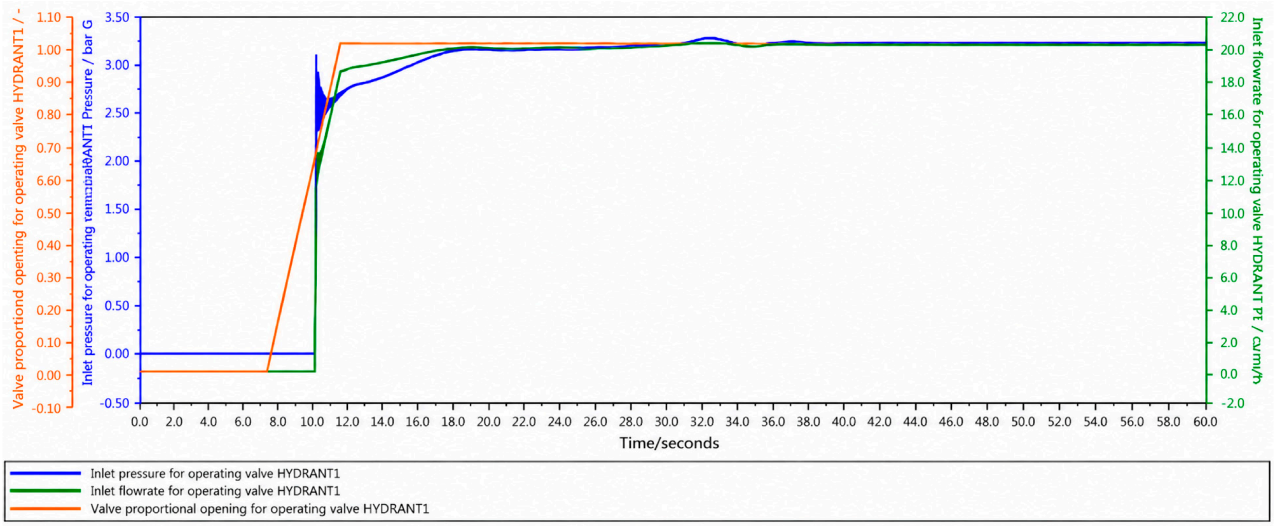

(**a**)

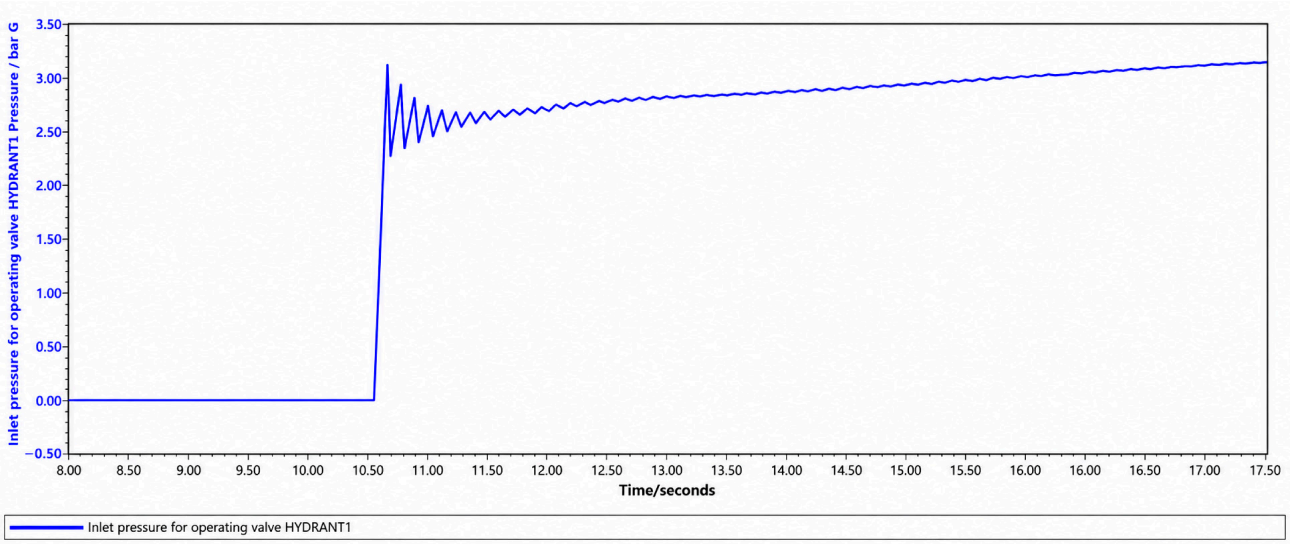

(**b**)

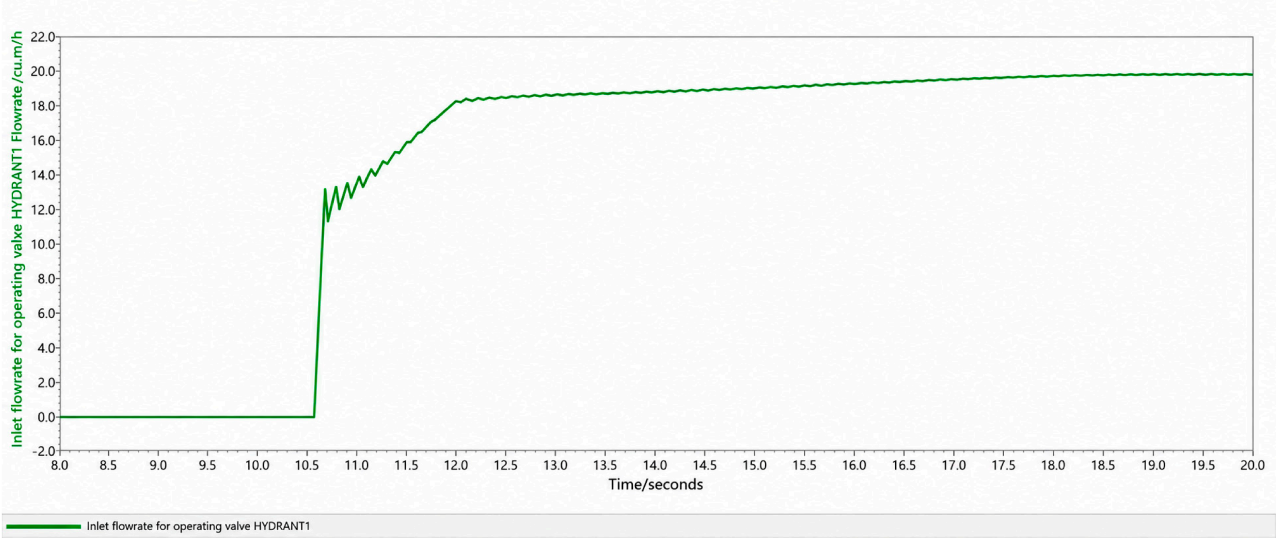

(**c**)

Figure 9. Transient response of the hydrant branch during Case I for the modified PSV arrangement: (**a**) overall hydraulic response; (**b**) inlet-pressure evolution; (**c**) inlet-flow-rate evolution.

The hydrant branch maintains stable operating conditions following the initial transient period. The pressure and flow-rate curves show that the modified arrangement does not introduce additional oscillations or reduce the hydraulic availability of the branch. The hydrant branch therefore remains hydraulically available following the initial transient, while benefiting from the faster attenuation of the pressure waves generated during pump start-up and deluge valve opening.

At the network level, the governing maximum pressure decreases from 17.602 barg in the original configuration to 16.936 barg after modification. This corresponds to a reduction of approximately 3.8%, with the modified maximum remaining below the adopted allowable limit of 17.5 barg. The corresponding governing maxima were recorded at the inlet of Pipe 50 at approximately t = 33.784 s in the original configuration and at the outlet of Main Fire Pump A at approximately t = 33.368 s in the modified configuration. The minimum network pressure changes from −0.013 barg in the original configuration, occurring at the outlet of Pipe 77 at approximately t = 4.564 s, to −0.624 barg in the modified configuration, occurring at the inlet of Pipe 14 at approximately t = 4.444 s. Although this value is lower than that obtained for the original configuration, it remains above the adopted vapour-pressure limit of −0.971 barg; therefore, no indication of vapour-cavity formation or liquid-column separation is obtained within the present single-phase model.

Overall, Case I demonstrates that relocating the check valve and reducing the PSV set pressure improve overpressure control and shorten the pump stabilisation period while maintaining stable hydraulic operation of the activated firefighting branches. Although the minimum network pressure decreases from approximately −0.013 barg to −0.624 barg, it remains above the adopted vapour-pressure limit of −0.971 barg. The modified configuration therefore provides improved control of the positive-pressure transient while maintaining an acceptable minimum-pressure margin.

3.2. Transient Hydraulic Response During Case II

Case II investigates the hydraulic transient generated by the controlled closure of the deluge valve while Main Fire Pump A remains in continuous operation. Unlike Case I, the pump is already operating when the transient event begins; therefore, the pressure waves are generated primarily by flow deceleration and the progressive increase in hydraulic resistance associated with valve closure.

The deluge valve is initially fully open and begins to close at t = 2 s. The closure is completed at t = 7 s, corresponding to a closing time of 5 s. Main Fire Pump A operates continuously throughout the simulation, whereas the jockey pump is excluded from the model. The hydrants and fire monitor remain closed to isolate the hydraulic effects generated by the deluge valve operation. The transient response of the main fire pump for the original and modified configurations is compared in Figure 10.

In the original configuration, the pump initially operates at a discharge pressure of approximately 16.2 barg, a suction pressure of approximately 1.27 barg and a discharge flow rate of approximately 2500 m^3/h. As the deluge valve closes, the reduction in system demand shifts the pump operating point towards lower flow and higher-pressure conditions. Consequently, the discharge flow rate decreases to approximately 1300 m^3/h, while the discharge pressure reaches a maximum of approximately 17.8 barg.

The suction pressure increases to approximately 1.51 barg before stabilising at approximately 1.48 barg. After valve closure, the suction and discharge pressures exhibit persistent oscillations, while the discharge flow rate remains practically constant. This behaviour indicates that the pump reaches a new operating regime but continues to be affected by pressure waves propagating through the firewater ring main.

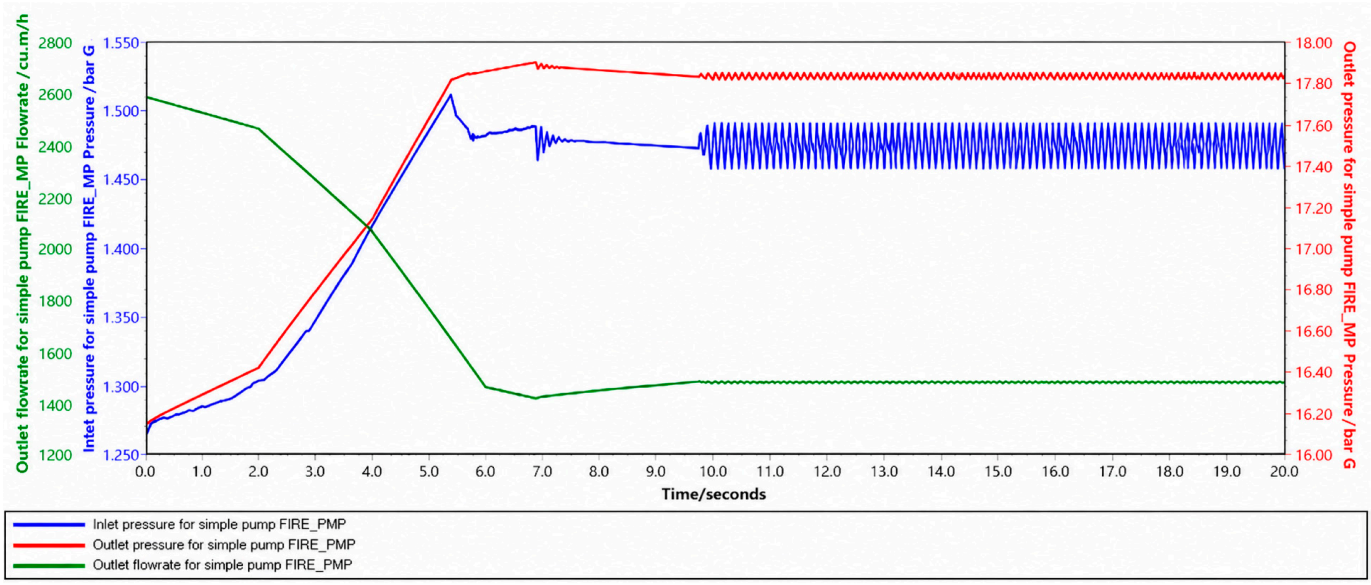

(**a**)

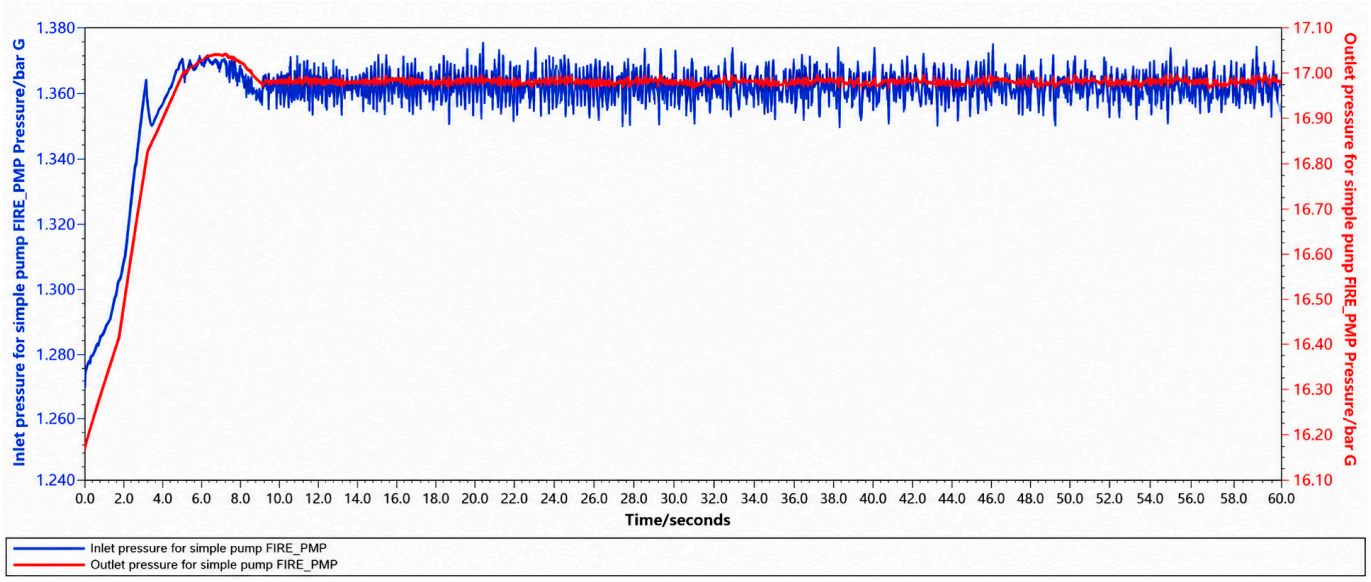

(**b**)

Figure 10. Transient response of the fire pump during Case II: (**a**) original configuration; (**b**) modified PSV arrangement.

Under the modified configuration, the discharge flow rate remains approximately 1300 m^3/h, demonstrating that the proposed optimisation does not reduce the hydraulic capacity available from the pump. However, the stabilised suction pressure decreases from approximately 1.48 barg to 1.36 barg, representing a reduction of approximately 8.1%, while the discharge pressure decreases from approximately 17.8 barg to 17.0 barg, corresponding to a reduction of approximately 4.5%. The pressure oscillations are also attenuated, confirming the beneficial influence of the modified PSV arrangement on the pump response. Transient response of the deluge valve during Case II is presented in Figure 11.

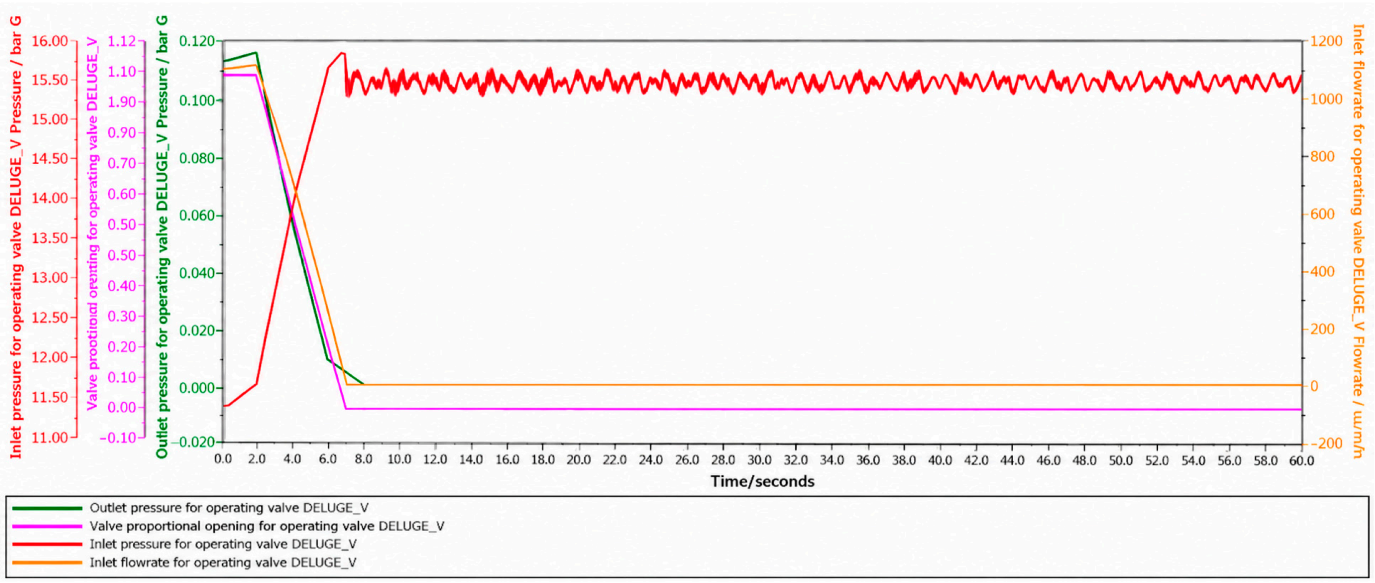

(**a**)

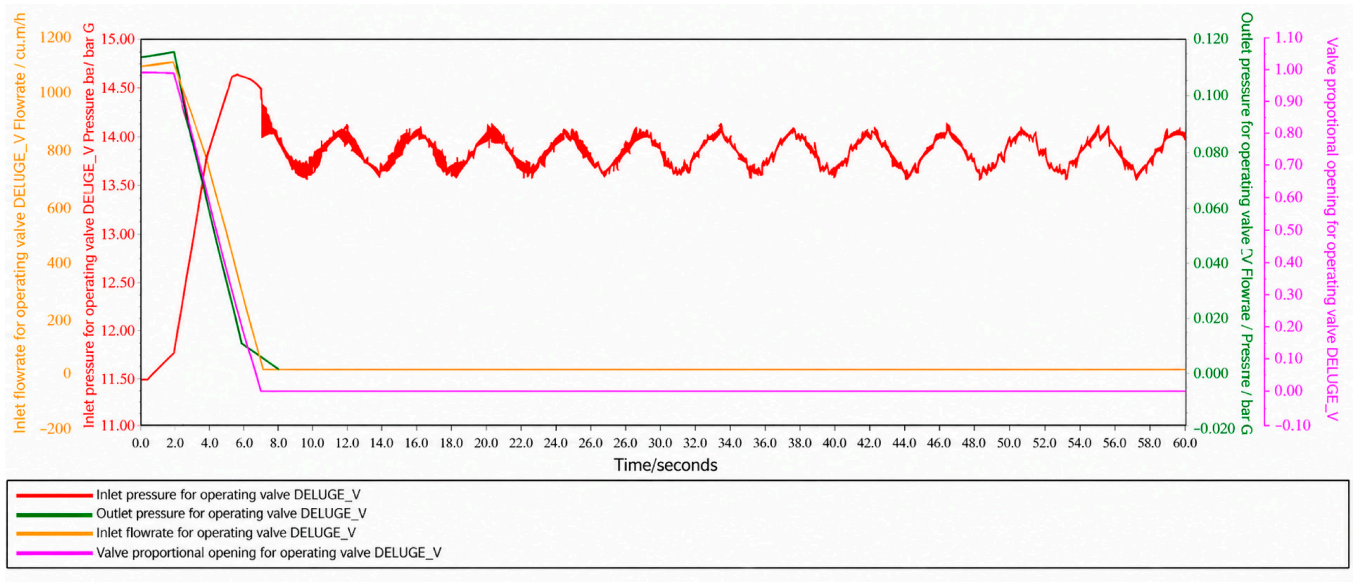

(**b**)

Figure 11. Transient response of the deluge valve during Case II: (**a**) original configuration; (**b**) modified PSV arrangement.

At the beginning of the simulation, the deluge valve is fully open, with an inlet pressure of approximately 11.3 barg, an outlet pressure of approximately 0.115 barg and an inlet flow rate close to 1100 m^3/h. During the 5 s closure sequence, the valve opening decreases progressively from 100% to 0%, producing a complete interruption of flow through the deluge branch.

As the valve closes, the inlet flow rate decreases from approximately 1100 m^3/h to zero, while the outlet pressure decreases to approximately 0 barg. In contrast, the inlet pressure rises rapidly to approximately 15.8 barg before stabilising at approximately 15.5 barg. The maximum inlet pressure is therefore approximately 40% higher than the initial value. Low-amplitude pressure oscillations persist upstream of the valve after complete closure, demonstrating that isolating the downstream branch does not immediately dissipate the transient energy accumulated within the ring main.

The modified pressure-protection arrangement reduces the maximum pressure level, while post-closure pressure oscillations remain visible. The maximum pressure above the Main Deck decreases from 15.8 barg to 14.6 barg, corresponding to a reduction of approximately 7.6%. The optimised value remains below the allowable pressure of 15.5 barg specified for the piping located above the Main Deck. The transmission of the pressure disturbance towards the hydrant branch is compared in Figure 12.

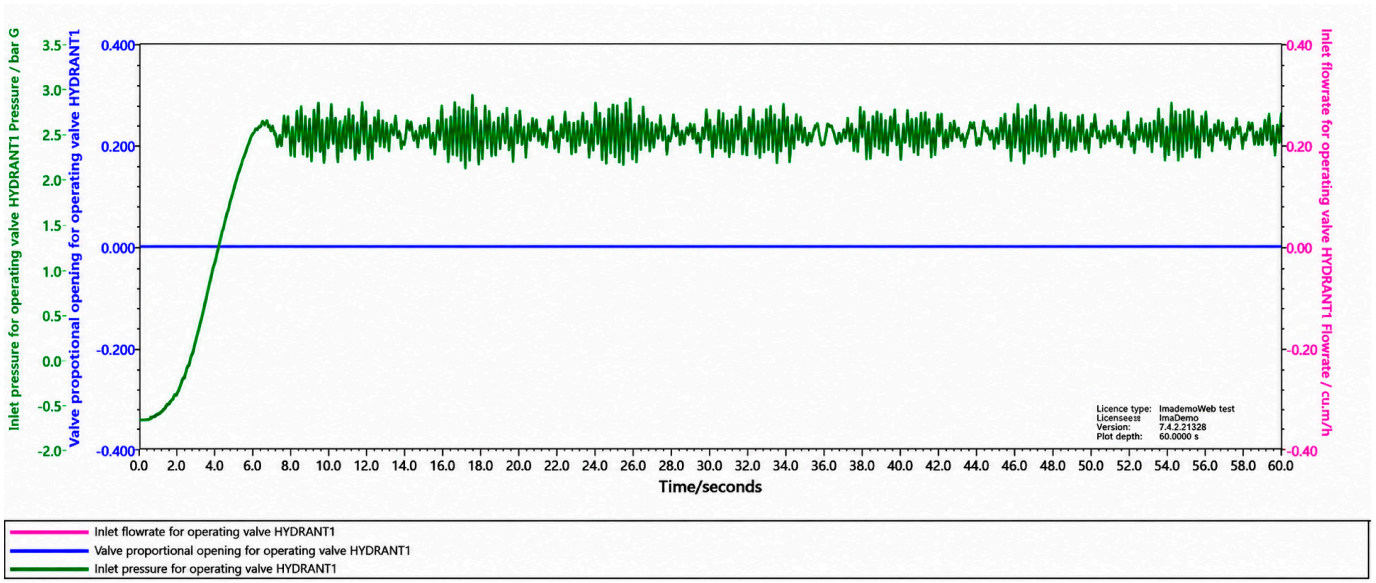

(**a**)

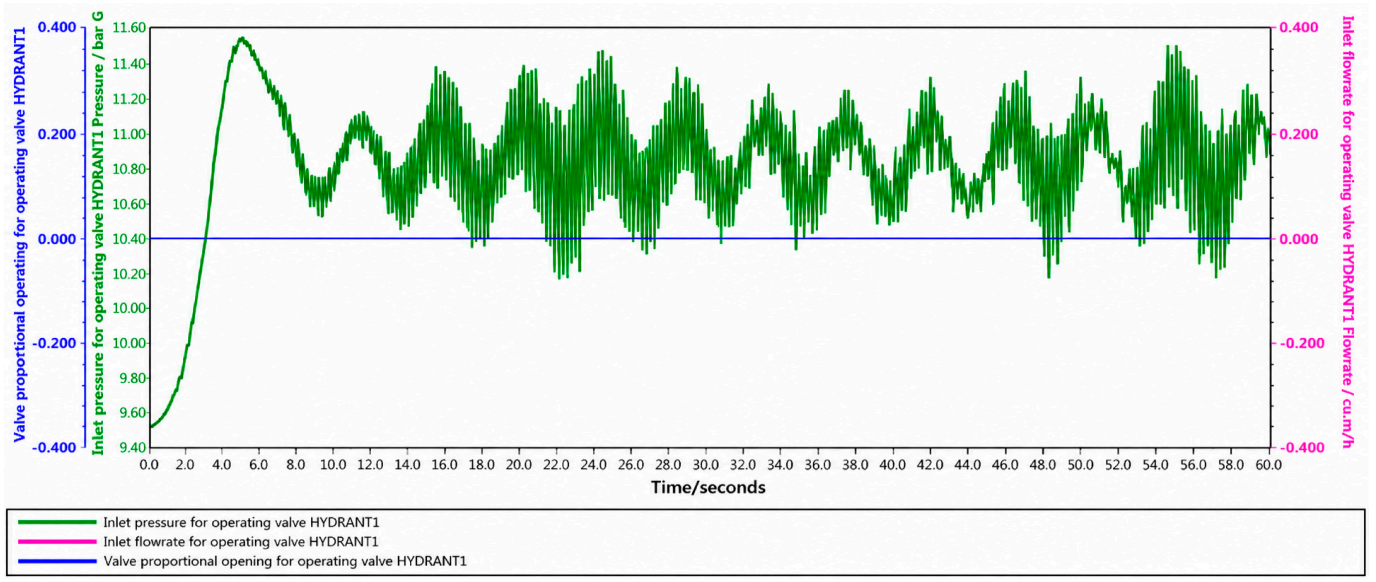

(**b**)

Figure 12. Transient response of the hydrant branch during Case II: (**a**) original configuration; (**b**) modified PSV arrangement.

Although the hydrants remain closed during Case II, their location is relevant because they represent hydraulically remote and elevated points of the firewater network. In both configurations, the pressure at the monitored hydrant branch remains well above the adopted vapour-pressure threshold. The global minimum pressure within the complete network is approximately 1.3 barg in both configurations and occurs at approximately t = 0.2 s at the same elevated ring-main location. The hydrant-branch pressure histories therefore illustrate the transmission of the transient disturbance towards a remote part of

the network, while hydraulic acceptability is assessed using the governing network-level pressure extrema.

At the network level, the original configuration generates a maximum pressure of 15.8 barg above the Main Deck and 18.6 barg below the Main Deck. These values exceed the corresponding allowable limits of 15.5 barg and 17.5 barg, respectively. The most significant exceedance occurs below the Main Deck, where the calculated pressure is 1.1 barg above the design limit.

After relocating the check valve and reducing the PSV set pressure from 17.5 barg to 16.5 barg, the maximum pressure above the Main Deck decreases to 14.6 barg, while the maximum pressure below the Main Deck decreases to 17.04 barg. The latter represents a reduction of approximately 8.4% relative to the original value of 18.6 barg. Both maximum pressures therefore remain within the applicable design limits after optimisation.

Overall, Case II demonstrates that closure of the deluge valve produces a substantial conversion of flow kinetic energy into pressure energy, resulting in pressure peaks and sustained oscillations throughout the firewater network. The original pressure protection arrangement is insufficient to maintain the maximum pressures within the design envelope. In contrast, the modified PSV arrangement reduces the governing pressure peaks, attenuates pressure oscillations and preserves the required pump flow rate. The optimisation therefore restores compliance with the allowable pressure limits without producing pressures below the adopted vapour-pressure threshold in the present single-phase model and without adversely affecting the hydraulic availability of the firewater system.

3.3. Transient Hydraulic Response During Case III

Case III investigates the hydraulic transient generated by the closure of the fire monitor while Main Fire Pump A remains in continuous operation. This scenario was selected to evaluate whether the rapid interruption of flow through a local firefighting branch can generate critical pressure variations within the interconnected firewater ring main.

At the beginning of the simulation, the fire monitor is fully open and receives a flow rate of approximately 120 m^3/h. The monitor remains fully open until approximately t = 2 s and subsequently closes between t = 2 s and t = 4 s, corresponding to a closing duration of approximately 2 s. The main fire pump remains operational throughout the simulation, while the deluge system and the two hydrants remain closed. The scheduled event of interest is the interruption of flow through the monitor branch; however, the complete simulation interval also includes the initial hydraulic state and the associated network response before monitor closure begins.

The archived PIPENET pressure-extrema report for the original Case III configuration records a maximum pressure of 19.318 barg in Pipe 58, at 2.486 m from its inlet, at t = 0.098 s. The minimum pressure is −6.269 barg in Pipe 54, at 57.77 m from its inlet, at t = 0.140 s. These values exceed the adopted upper pressure limit of 17.5 barg below the Main Deck and fall below the vapour-pressure threshold of −0.971 barg, respectively. The negative value is interpreted as an indication that the single-phase calculation exceeds its physical applicability, rather than as a physically sustainable liquid pressure.

Both extrema occur before the scheduled monitor-closing operation, which begins at t = 2 s. Accordingly, these values are treated as the governing extrema of the complete recorded simulation interval and are not attributed directly to the monitor-closure operation. The physical origin of these pre-event extrema cannot be reconstructed conclusively from the available archived simulation records; consequently, they are retained for completeness as global extrema of the recorded Case III interval but are not used to characterise the direct effect of monitor closure. The transient response of the main fire pump for the original and modified configurations is compared in Figure 13.

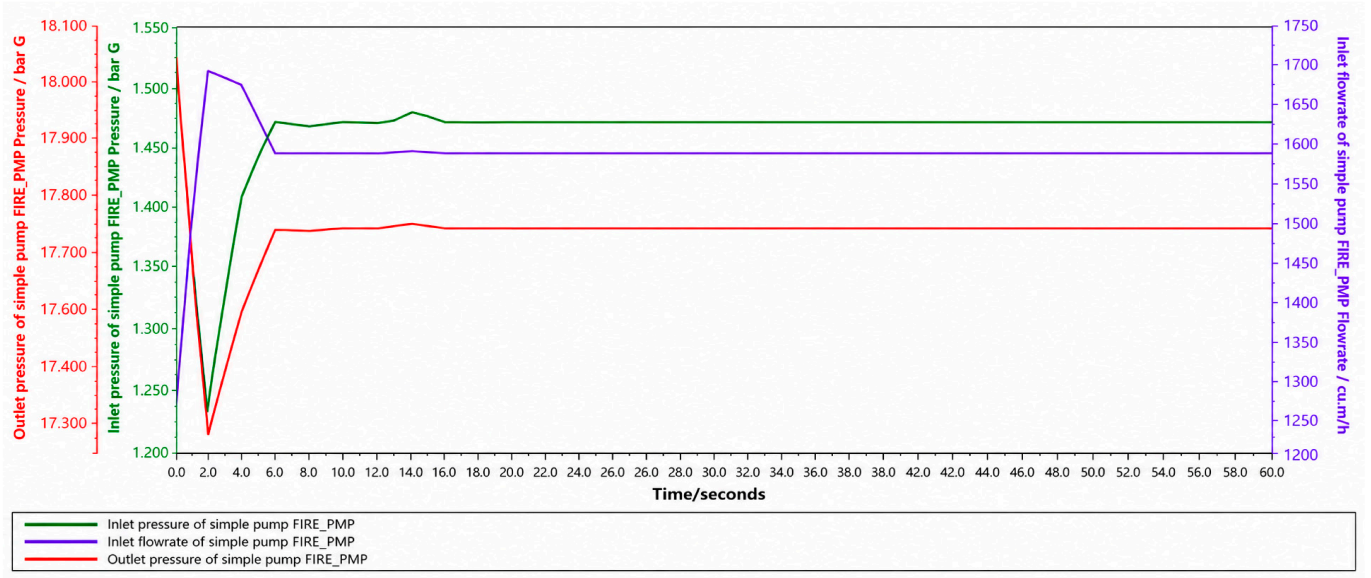

(**a**)

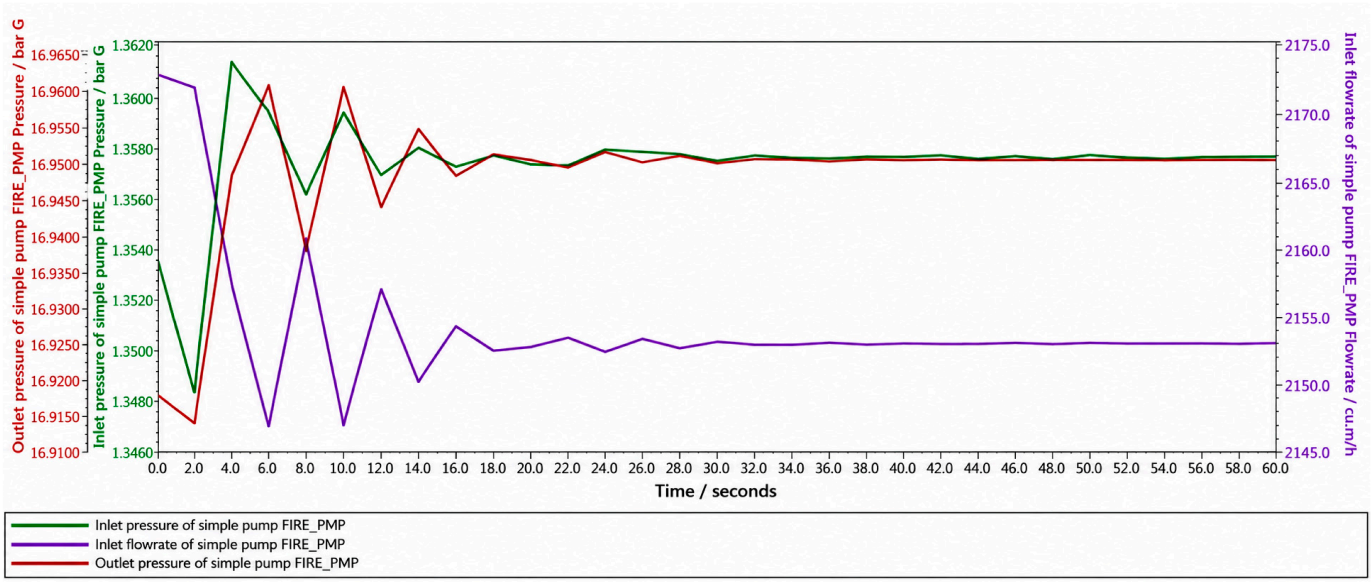

(**b**)

Figure 13. Transient response of the fire pump during Case III: (**a**) original configuration; (**b**) modified PSV arrangement.

In the original configuration, the fire pump initially delivers approximately 1700 m^3/h at a discharge pressure of approximately 17.95 barg and a suction pressure of approximately 1.50 barg. Immediately after monitor closure begins, the suction pressure decreases sharply to approximately 1.19 barg, corresponding to a reduction of approximately 21%. During the same interval, the discharge pressure decreases to approximately 17.35 barg, while the discharge flow rate decreases to approximately 1600 m^3/h.

The pump parameters subsequently recover as the system approaches a new hydraulic equilibrium. The suction pressure stabilises at approximately 1.46 barg, while the discharge pressure stabilises at approximately 17.82 barg. The discharge flow rate remains practically constant at approximately 1600 m^3/h. The pressure and flow-rate histories indicate that the pump approaches a relatively stable operating regime within approximately 6–8 s in the original configuration. However, the extreme pressure values recorded in the

downstream network demonstrate that stable conditions at the pump do not necessarily indicate acceptable transient behaviour throughout the firewater system.

To mitigate these effects, the check valve was relocated immediately downstream of the main pump discharge flange and upstream of the PSV. The PSV set pressure was simultaneously reduced from 17.5 barg to 16.5 barg. All other model parameters, boundary conditions and operating sequences remained unchanged.

Following optimisation, the stabilised pump flow rate increases from approximately 1600 m^3/h to 2150 m^3/h, representing an increase of approximately 34%. This increase does not represent additional demand from the fire monitor; rather, it reflects the different hydraulic operating point established by the modified pressure-protection configuration. The suction pressure stabilises at approximately 1.36 barg, compared with approximately 1.46 barg in the original configuration, while the discharge pressure decreases from approximately 17.82 barg to 16.95 barg, corresponding to a reduction of approximately 4.9%.

In the modified configuration, the pressure and flow-rate histories approach their final operating regime over approximately 15–20 s, compared with approximately 6–8 s for the original configuration. These values are therefore interpreted as approximate settling ranges observed from the calculated histories. The proposed modification does not produce a shorter settling response in Case III. Nevertheless, the amplitudes of the suction- and discharge-pressure oscillations are reduced by more than 90%, resulting in a substantially smoother and less severe pump response. This demonstrates that stabilisation time alone is insufficient for evaluating the effectiveness of a surge-protection measure; the amplitude of the transient pressure variations and the resulting pressure envelope must also be considered. The hydraulic response measured directly at the fire monitor is presented in Figure 14.

In both configurations, the fire monitor remains fully open until approximately t = 2 s and closes completely by approximately t = 4 s, corresponding to a closing duration of approximately 2 s, while its inlet flow rate decreases from approximately 120 m^3/h to zero. The proposed modification therefore does not alter the required closing sequence or the complete hydraulic isolation of the monitor branch.

In the original configuration, the monitor inlet pressure reaches a local maximum of approximately 15.4 barg at t = 4 s. It then decreases gradually towards approximately 14.9 barg at the end of the simulation, with small residual oscillations.

In the modified configuration, the monitor inlet pressure increases from approximately 13.7 barg to a local maximum of approximately 14.4 barg at t = 4 s. Subsequently, persistent pressure oscillations are observed, generally ranging between approximately 13.7 and 14.1 barg over the remainder of the simulation. The modification therefore reduces the local maximum pressure at the monitor inlet, although post-closure oscillations remain visible. This local response must be distinguished from the governing pressure extrema calculated throughout the network.

The beneficial influence of the modified arrangement is also observed in the inactive deluge and hydrant branches. At the deluge valve, the pressure excursion decreases from approximately 1.15 bar to less than 0.30 bar, representing a reduction of approximately 75%. At the hydrant branch, the pressure variation decreases from approximately 3.4 bar to less than 0.40 bar, corresponding to a reduction of approximately 88%. Thus, the proposed changes substantially reduce the pressure excursions transmitted to the inactive deluge and hydrant branches and lower the local maximum pressure at the monitor inlet, although post-closure oscillations remain visible.

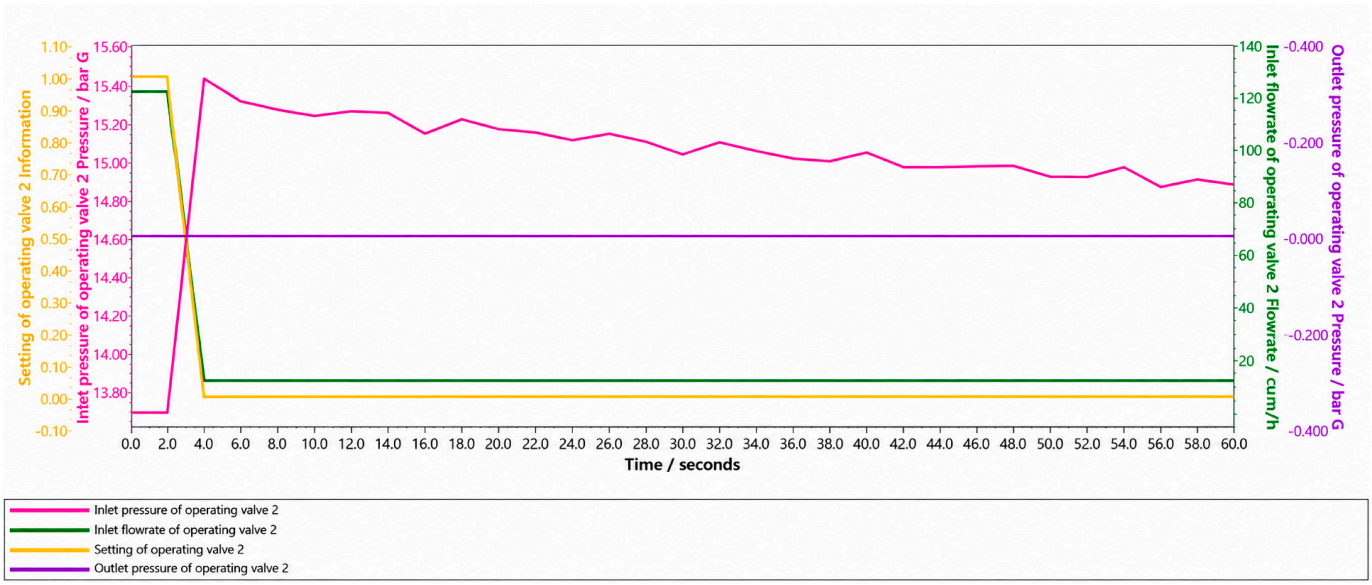

(**a**)

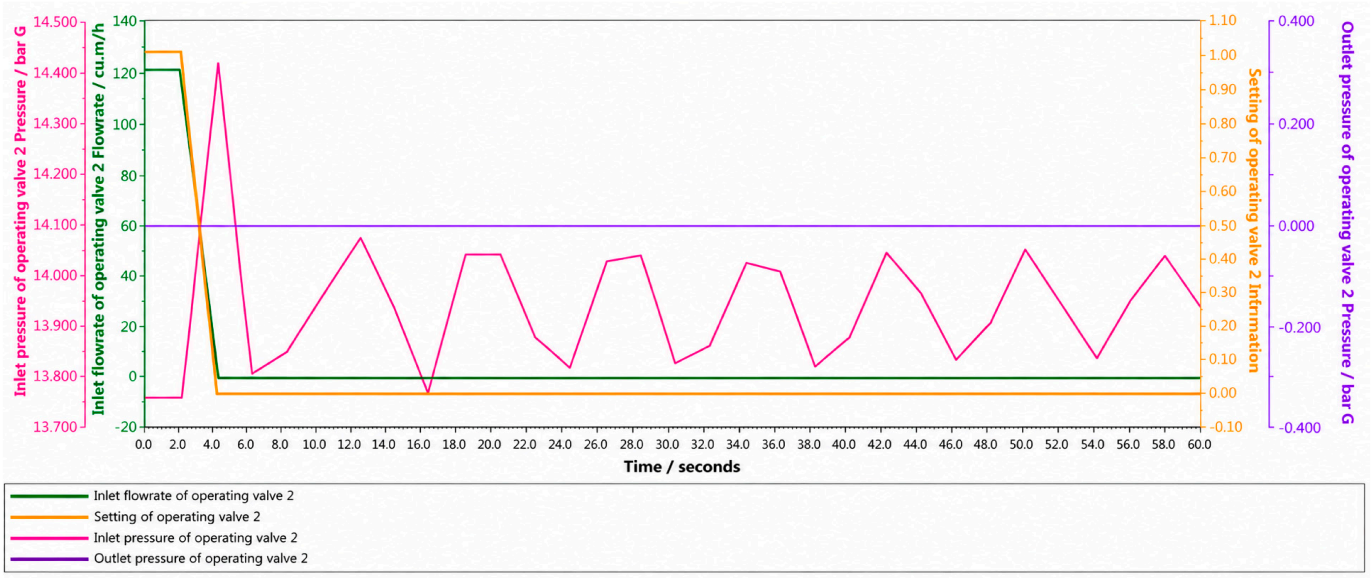

(**b**)

Figure 14. Transient response of the fire monitor during Case III: (**a**) original configuration; (**b**) modified PSV arrangement.

At the system level, the maximum pressure below the Main Deck decreases from 19.318 barg in the original configuration to 16.974 barg in the modified configuration, representing a reduction of approximately 12.1%. More precisely, for the modified configuration, the governing maximum pressure was approximately 16.97 barg and occurred at the outlet of Main Fire Pump A at approximately t = 4.881 s. The resulting maximum pressure remains below the allowable limit of 17.5 barg. The minimum pressure simultaneously increases from −6.2 barg in the original configuration to 0.0 barg in the modified configuration, thereby substantially improving the minimum-pressure margin within the complete simulation interval.

Overall, Case III exhibited the widest pressure envelope among the investigated simulations. In the original configuration, the governing maximum and minimum pressures over the complete simulation interval were approximately 19.3 barg and −6.27 barg, respectively. Following modification, these extrema were limited to approximately 16.97 barg and

0.0 barg. The modified arrangement therefore substantially reduced the overall pressure excursions and attenuated the pressure oscillations transmitted throughout the network. Because the governing extrema of the original configuration occurred before the scheduled monitor closure, they should not be interpreted solely as a direct consequence of that operation.

3.4. Comparative Assessment of the Investigated Scenarios

The three investigated scenarios generate different transient responses because they involve distinct mechanisms of flow acceleration and deceleration. Case I combines main fire pump start-up with deluge valve opening, Case II considers the progressive closure of the deluge valve during continuous pump operation, and Case III examines the rapid closure of the fire monitor. The governing pressure extrema were further examined using the PIPENET pressure-envelope and observed-extrema outputs. For each configuration, the governing minimum and maximum transient pressures, together with the available location and occurrence-time information from the archived PIPENET outputs, are summarised in Table 5.

Table 5. Comparison of the principal transient results for the investigated scenarios.

Case	Configuration	Minimum Pressure (Barg)	Location of Minimum	Time (s)	Governing Maximum Pressure (Barg)	Location of Maximum	Time (s)
Case I	Original	−0.013	Pipe 77, outlet	4.564	17.602	Pipe 50, inlet	33.784
Case I	Modified	−0.624	Pipe 14, inlet	4.444	16.936	Fire Pump A, outlet	33.368
Case II	Original	1.3	Elevated ring-main location (global minimum-pressure point)	0.2	18.6	Below Main Deck, governing pressure-envelope location	≈10
Case II	Modified	1.3	Elevated ring-main location (global minimum-pressure point)	0.2	17.04	Below Main Deck, governing pressure-envelope location	7
Case III	Original	−6.269	Pipe 54, 57.77 m from inlet	0.140	19.318	Pipe 58, 2.486 m from inlet	0.098
Case III	Modified	0.000	Pipe 54, outlet	0.000	16.974	Fire Pump A, outlet	4.881

Note: The calculated minimum pressure of −6.2 barg indicates that the numerical solution falls below the vapour-pressure threshold. This value should be interpreted as an indicator of transient cavitation and possible liquid-column separation, rather than as a physically sustainable liquid pressure. For Case II, the archived pressure-envelope output did not permit retrospective component-level identification of the governing extrema; therefore, the corresponding locations are reported at the available network level. For the original Case II maximum, the archived output supported only an approximate occurrence time, which is therefore reported as ≈10 s.

The allowable minimum pressure adopted in the analysis is −0.971 barg, while the maximum allowable pressure below the Main Deck is 17.5 barg.

Case I produces the least severe transient response among the three original configurations. The maximum pressure below the Main Deck reaches 17.6 barg, exceeding the allowable limit by only 0.1 barg. The minimum pressure remains above the vapour-pressure limit in both configurations. Following optimisation, the maximum pressure decreases to 16.936 barg, while the pump stabilisation time decreases from approximately

35 s to 20 s. Therefore, the principal benefit of the modification in Case I is the attenuation of the pump-start-up transient and the reduction in the time required to establish stable firefighting flow.

Case II generates a more pronounced overpressure because closure of the deluge valve converts the kinetic energy of the flowing water into pressure energy. In the original configuration, the maximum pressure below the Main Deck reaches 18.6 barg, exceeding the allowable limit by 1.1 barg. The minimum pressure remains positive and above the adopted vapour-pressure threshold; therefore, no cavitation indication is obtained within the present single-phase model for this scenario. After optimisation, the maximum pressure decreases to 17.04 barg, representing a reduction of approximately 8.4%, while the minimum pressure remains approximately 1.3 barg in both configurations. Case II is therefore governed by the maximum-pressure criterion rather than by the risk of underpressure.

Case III exhibits the most severe global pressure extrema among the original simulations. The complete simulation interval includes a maximum pressure of approximately 19.3 barg below the Main Deck and a minimum pressure of approximately −6.27 barg. Both values lie outside the adopted pressure envelope. As discussed in Section 3.3, however, these extrema occur before the scheduled monitor closure and therefore cannot be attributed directly to that operation. They are consequently used here as global Case III extrema for comparison between the original and modified configurations.

Following modification of the pressure-protection arrangement, the maximum pressure decreases to approximately 16.97 barg and the minimum calculated pressure increases to 0.0 barg. Both values lie within the adopted pressure limits. Case III therefore shows the largest reduction in the overall pressure envelope among the investigated simulations.

The results demonstrate that the severity of a system-level pressure envelope cannot be inferred solely from the nominal flow rate of the affected consumer. Event timing, network state, pressure-wave propagation and component interactions must also be considered when comparing transient operating cases.

The results also show that the effects of the modified arrangement differ between the investigated scenarios. For Case I, the principal improvements are faster pump stabilisation and reduced maximum pressure. For Case II, the optimisation mainly controls the overpressure produced by deluge valve closure. For Case III, the modified arrangement reduces the governing maximum pressure and raises the calculated minimum pressure above the adopted vapour-pressure threshold.

Overall, relocating the check valve immediately downstream of the fire pump and reducing the PSV set pressure from 17.5 barg to 16.5 barg bring all three investigated scenarios within the adopted pressure limits. The modified arrangement therefore provides a consistent pressure-surge mitigation strategy for both pump-driven and valve-driven transient events. Nevertheless, the strong differences observed between the three cases confirm that offshore firewater systems should be assessed using multiple representative emergency sequences rather than a single governing assumption.

3.5. Engineering Interpretation and Comparison with Previous Studies

The numerical results confirm that transient severity in a complex firewater network cannot be assessed solely from the nominal flow rate of the affected consumer. The response depends on the rate of flow variation, component-operating time, network topology, wave reflections and interaction between the initiating component and the pressure-protection arrangement.

In Case I, the simultaneous opening of the deluge valve and start-up of the main fire pump generates a comparatively moderate pressure exceedance but a relatively long stabilisation period. The pressure response is governed by the progressive acceleration of

the water column and the movement of the pump operating point while several firefighting consumers become active. This behaviour is consistent with classical transient theory, according to which pump start-up produces a time-dependent interaction between the pump characteristic curve and the hydraulic resistance of the network [9–13].

In Case II, closure of the deluge valve over 5 s produces a substantial positive pressure surge but does not generate critical underpressure. Yuce and Omer [22] similarly demonstrated that valve-closing time and closure law have a major influence on the magnitude and shape of the resulting pressure waves. The present results extend this observation to a branched offshore firewater ring main, where the pressure disturbances continue to propagate after the downstream branch has been isolated.

A quantitative comparison further supports the influence of valve-operating characteristics on transient severity. Yuce and Omer [22] reported that, for linear valve closure in a stainless-steel pipeline, increasing the closure time by a factor of 50 reduced the maximum transient pressure head from 217.62 m to 84.77 m, corresponding to a reduction of approximately 61%. For the ductile pipeline investigated in the same study, the corresponding maximum pressure head decreased from 174.61 m to 83.43 m, representing a reduction of approximately 52%. Although the pipeline geometry, material properties and boundary conditions differ from those of the present FPSO firewater network, these results confirm the strong sensitivity of transient pressure to valve-closing time. In the present study, the 5 s deluge-valve closure in Case II generated a maximum pressure of 18.6 barg below the Main Deck, which was reduced to 17.04 barg after modification of the pressure-protection arrangement, corresponding to an 8.4% reduction. The smaller percentage reduction obtained in the present study should not be interpreted as a lower mitigation efficiency, since the two studies consider different network geometries, operating conditions and mitigation strategies.

Case III exhibits the widest pressure envelope among the investigated simulations. However, the archived global extrema occur before the scheduled monitor closure begins. The Case III results therefore cannot be used to attribute the maximum and minimum system pressures directly to interruption of the approximately 120 m^3/h monitor flow. Instead, they demonstrate the importance of evaluating the complete simulation interval and the overall network state when identifying the governing pressure envelope.

A particularly relevant quantitative comparison is provided by Park et al. [27], who investigated water-hammer behaviour in a seawater-treatment system installed on an offshore floating production unit using a one-dimensional Method-of-Characteristics model. Their parametric study showed that the use of equal-percentage valve characteristics reduced the pressure surge and oscillation amplitude by approximately 1–1.8 barg, while allowing the valve-closing time to be shortened by 10 s. In the present FPSO firewater network, the modified pressure-protection arrangement reduced the maximum pressure below the Main Deck by 1.56 barg in Case II, from 18.6 to 17.04 barg, and by approximately 2.35 barg in Case III, from 19.318 to 16.974 barg over the complete simulation interval. Although the mitigation mechanisms differ, the magnitude of the pressure reductions obtained in the present study is comparable with the surge attenuation reported by Park et al. [27].

The minimum pressure simultaneously increases from −6.2 barg to 0.0 barg. Since this value remains above the adopted seawater vapour-pressure threshold of −0.971 barg, the modified configuration removes the cavitation indication predicted by the present single-phase model. However, the model does not explicitly resolve vapour-cavity formation, growth or collapse. Previous experimental and numerical studies have shown that column separation can generate secondary pressure peaks when the separated liquid columns rejoin [14,16,21]. The calculated minimum pressure should therefore be interpreted as an indicator of cavitation risk rather than as a physically sustainable absolute liquid pressure.

The results also demonstrate the importance of check-valve location and closing behaviour. Sotoodeh [23] highlighted that check-valve selection and dynamic characteristics can substantially influence water-hammer loading in offshore piping. Detailed CFD studies have likewise shown that the pressure build-up generated during check-valve closure is sensitive to the valve motion and to the fluid velocity at the instant of complete closure [28]. In the investigated firewater network, relocating the check valve modifies pressure-wave transmission near the pump discharge and improves the effectiveness of the PSV.

The reduction of the PSV set pressure from 17.5 barg to 16.5 barg causes the protection device to activate earlier during transient overpressure. However, the improvement cannot be attributed only to the lower set pressure because the simultaneous relocation of the check valve changes the local hydraulic boundary conditions. The calculated response therefore represents the combined effect of the two modifications. Separate sensitivity simulations would be required to quantify their individual contributions.

The effectiveness of the modified arrangement varies between the three scenarios. In Case I, the principal benefits are reduced maximum pressure and faster pump stabilisation. In Case II, the modification reduces the overpressure caused by deluge-valve closure. In Case III, it simultaneously limits the maximum pressure and raises the calculated minimum pressure above the adopted vapour-pressure threshold, substantially reducing the cavitation susceptibility indicated by the present model. This scenario-dependent response supports the use of multiple operating cases when selecting and verifying surge-protection measures [9–12,26].

Compared with surge vessels or hydropneumatic tanks, the investigated modification does not require the addition of a large pressure-storage component. Hydropneumatic tanks can provide effective pressure-surge mitigation but require appropriate sizing, installation space and integration with the hydraulic system [26]. These considerations are particularly relevant on FPSO units, where equipment space and weight are constrained. Modifying the existing PSV arrangement may therefore provide a practical alternative when demonstrated to be effective for all relevant operating scenarios.

The use of a one-dimensional network model is appropriate for identifying critical system-level events and comparing alternative protection configurations. However, it does not resolve the local three-dimensional flow field within the valves or the structural response of the pipework. Recent reviews have shown that CFD can provide more detailed information regarding valve motion, turbulence and local pressure build-up but at substantially greater computational cost [24,25,28]. A combined approach could therefore use one-dimensional modelling for complete-network assessment and CFD or fluid–structure interaction analysis for selected critical components.

A principal contribution of the present study is the demonstration that different emergency operating cases can produce markedly different system-level pressure envelopes and that the governing extrema may occur outside the nominal actuation interval of the component under investigation. This finding would not be apparent from steady-state flow demand alone and confirms the need to assess the complete operating sequence and both limits of the transient pressure envelope during the design verification of offshore firewater systems.

4. Conclusions

This study evaluated the transient hydraulic response of an FPSO firewater ring-main system under three representative emergency operating scenarios. A one-dimensional model developed in PIPENET Vision Transient was used to compare the original system configuration with a modified pressure-protection arrangement involving relocation of the

check valve immediately downstream of the fire-pump discharge flange and reduction of the PSV set pressure from 17.5 barg to 16.5 barg.

The three operating sequences produced substantially different transient responses. In Case I, simultaneous fire-pump start-up and deluge-valve opening generated a maximum pressure of 17.6 barg below the Main Deck. The modified configuration reduced this value to 16.936 barg, corresponding to a reduction of approximately 3.8%, and decreased the estimated pump stabilisation time from approximately 35 s to 20 s.

In Case II, closure of the deluge valve while the main pump remained operational produced a maximum pressure of 18.6 barg below the Main Deck, exceeding the allowable limit of 17.5 barg. Following modification, the maximum pressure decreased to 17.04 barg, representing a reduction of approximately 8.4%. The minimum pressures remained above the adopted vapour-pressure threshold in both configurations; therefore, no cavitation indication was obtained within the present single-phase model for this scenario.

Case III exhibited the most severe pressure extrema among the investigated simulations. In the original configuration, the maximum and minimum pressures over the complete simulation interval were approximately 19.3 barg and −6.27 barg, respectively, whereas the modified configuration limited these extrema to approximately 16.97 barg and 0.0 barg. The comparison therefore indicates a substantial reduction in the overall pressure excursions in the modified system. The reported extrema refer to the complete simulation interval and should not be interpreted solely as the direct response to the scheduled monitor-closure event.

The comparative analysis demonstrates that transient severity cannot be inferred solely from the nominal flow rate of the affected consumer. Valve-operating time, rate of velocity variation, pressure-wave travel, component location and interaction with the complete network influence the resulting pressure envelope. Consequently, nominal consumer flow alone is insufficient to identify the governing system-level transient response, and the complete operating sequence must be considered.

The modified arrangement maintained the required hydraulic operation while bringing all three investigated scenarios within the adopted maximum- and minimum-pressure limits. Relocating the check valve and reducing the PSV set pressure therefore provide an effective surge-mitigation strategy for the investigated firewater network. Because both modifications were introduced simultaneously, additional sensitivity simulations would be required to quantify their individual contributions.

The results also confirm that steady-state calculations alone are insufficient for verifying offshore firewater systems. Transient analysis should be integrated into the design process to identify critical operating sequences, evaluate pressure-protection devices and detect local underpressure conditions that may not be apparent from nominal pump and consumer data.

The study is limited by its one-dimensional numerical representation and the absence of full-scale experimental measurements. Fluid–structure interaction, detailed valve dynamics, multiphase cavity behaviour and local three-dimensional flow structures were not explicitly resolved. Future work should therefore include model calibration using pressure measurements, separate assessment of the check-valve relocation and PSV set-point reduction, sensitivity analyses of valve-operating times and higher-fidelity simulations of the components governing the most severe transient events.

Author Contributions: Conceptualization, O.S.D.; methodology, O.S.D.; software, O.S.D.; formal analysis, R.B.; investigation, O.S.D. and R.B.; validation, O.S.D., R.B. and C.U.; writing—original draft preparation, O.S.D. and R.B.; writing—review and editing, C.U.; supervision, C.U. All authors have read and agreed to the published version of the manuscript.

Funding: This research received no external funding.

Institutional Review Board Statement: Not applicable.

Informed Consent Statement: Not applicable.

Data Availability Statement: The original contributions presented in this study are included in the article; further inquiries can be directed to the corresponding author.

Acknowledgments: The authors gratefully acknowledge ICEPRONAV Engineering SRL for its valuable technical support and assistance during this study. The authors also acknowledge the technical support and research facilities provided by the Naval Architecture Research Center of the Faculty of Naval Architecture, "Dunarea de Jos" University of Galati.

Conflicts of Interest: The author Oana Stefania Damian is employed by ICEPRONAV Engineering SRL. The remaining authors declare that the research was conducted in the absence of any commercial or financial relationships that could be construed as a potential conflict of interest.

Abbreviations

The following abbreviations are used in this manuscript:

CAD	Computer-Aided Design
CFD	Computational Fluid Dynamics
FPSO	Floating Production Storage and Offloading
GA	General Arrangement
GRE	Glass-Reinforced Epoxy
MOC	Method of Characteristics
P&ID	Piping and Instrumentation Diagram
PSV	Pressure Safety Valve
RTRP	Reinforced Thermosetting Resin Pipe
Symbols	
A	Pipe cross-sectional area in m^2
a	Pressure-wave propagation velocity in m/s
D	Pipe internal diameter in m
f	Darcy–Weisbach friction factor
g	Gravitational acceleration in m/s^2
H	Hydraulic head in m
K_v	Metric valve flow coefficient in $m^3\ h^{-1}\ bar^{-1}/^2$
Q	Volumetric flow rate in m^3/s
t	Time in s
x	Distance along the pipe in m
ΔP	Transient pressure variation in Pa
ΔV	Change in flow velocity in m/s
ρ	Fluid density in kg/m^3
R	Relative change produced by the modified configuration in %
X_{orig}	Value obtained for the original configuration
X_{mod}	Value obtained for the modified configuration

References

1. Bhardwaj, U.; Teixeira, A.P.; Guedes Soares, C.; Ariffin, A.K.; Singh, S.S. Evidence-based risk analysis of fire and explosion accident scenarios in FPSOs. *Reliab. Eng. Syst. Saf.* **2021**, *215*, 107904. [CrossRef]
2. Xie, X.; Xiong, Y.; Xie, W.; Li, J.; Zhang, W. Quantitative risk analysis of oil and gas fires and explosions for FPSO systems in China. *Processes* **2022**, *10*, 902. [CrossRef]
3. *ISO 13702:2024*; Oil and Gas Industries—Control and Mitigation of Fires and Explosions on Offshore Production Installations—Requirements and Guidelines, 3rd ed. ISO (International Organization for Standardization): Geneva, Switzerland, 2024.

4. International Maritime Organization. *SOLAS—International Convention for the Safety of Life at Sea: Consolidated Edition 2024*; IMO: London, UK, 2024.
5. International Maritime Organization. *International Code for Fire Safety Systems (FSS Code)*, 2015th ed.; IMO: London, UK, 2015.
6. *NFPA 15*; Standard for Water Spray Fixed Systems for Fire Protection, 2022nd ed. NFPA (National Fire Protection Association): Quincy, MA, USA, 2022.
7. *NFPA 20*; Standard for the Installation of Stationary Pumps for Fire Protection, 2022nd ed. NFPA (National Fire Protection Association): Quincy, MA, USA, 2022.
8. *NFPA 24*; Standard for the Installation of Private Fire Service Mains and Their Appurtenances, 2022nd ed. NFPA (National Fire Protection Association): Quincy, MA, USA, 2022.
9. Chaudhry, M.H. *Applied Hydraulic Transients*, 3rd ed.; Springer: New York, NY, USA, 2014. [CrossRef]
10. Wylie, E.B.; Streeter, V.L.; Suo, L. *Fluid Transients in Systems*; Prentice Hall: Englewood Cliffs, NJ, USA, 1993.
11. Thorley, A.R.D. *Fluid Transients in Pipeline Systems*, 2nd ed.; Professional Engineering Publishing: London, UK, 2004.
12. Larock, B.E.; Jeppson, R.W.; Watters, G.Z. *Hydraulics of Pipeline Systems*; CRC Press: Boca Raton, FL, USA, 2000.
13. Ghidaoui, M.S.; Zhao, M.; McInnis, D.A.; Axworthy, D.H. A review of water hammer theory and practice. *Appl. Mech. Rev.* **2005**, *58*, 49–76. [CrossRef]
14. Bergant, A.; Simpson, A.R.; Tijsseling, A.S. Water hammer with column separation: A historical review. *J. Fluids Struct.* **2006**, *22*, 135–171. [CrossRef]
15. Bergant, A.; Tijsseling, A.S.; Vítkovský, J.P.; Covas, D.I.C.; Simpson, A.R.; Lambert, M.F. Parameters affecting water-hammer wave attenuation, shape and timing—Part 1: Mathematical tools. *J. Hydraul. Res.* **2008**, *46*, 373–381. [CrossRef]
16. Bergant, A.; Tijsseling, A.S.; Vítkovský, J.P.; Covas, D.I.C.; Simpson, A.R.; Lambert, M.F. Parameters affecting water-hammer wave attenuation, shape and timing—Part 2: Case studies. *J. Hydraul. Res.* **2008**, *46*, 382–391. [CrossRef]
17. Tijsseling, A.S. Fluid–structure interaction in liquid-filled pipe systems: A review. *J. Fluids Struct.* **1996**, *10*, 109–146. [CrossRef]
18. Zielke, W. Frequency-dependent friction in transient pipe flow. *J. Basic Eng.* **1968**, *90*, 109–115. [CrossRef]
19. Vardy, A.E.; Brown, J.M.B. Transient turbulent friction in smooth pipe flows. *J. Sound Vib.* **2003**, *259*, 1011–1036. [CrossRef]
20. Covas, D.; Stoianov, I.; Ramos, H.; Graham, N.; Maksimović, Č. The dynamic effect of pipe-wall viscoelasticity in hydraulic transients. Part I—Experimental analysis and creep characterization. *J. Hydraul. Res.* **2004**, *42*, 516–530. [CrossRef]
21. Zhao, L.; Yang, Y.; Wang, T.; Han, W.; Wu, R.; Wang, P.; Wang, Q.; Zhou, L. An experimental study on the water hammer with cavity collapse under multiple interruptions. *Water* **2020**, *12*, 2566. [CrossRef]
22. Yuce, M.I.; Omer, A.F. Hydraulic transients in pipelines due to various valve closure schemes. *SN Appl. Sci.* **2019**, *1*, 1110. [CrossRef]
23. Sotoodeh, K. The mathematical analysis and review of water hammering in check valves in offshore industry. *J. Inst. Eng. Ser. C* **2023**, *104*, 879–885. [CrossRef]
24. Pal, S.; Hanmaiahgari, P.R.; Karney, B.W. An overview of the numerical approaches to water hammer modelling: The ongoing quest for practical and accurate numerical approaches. *Water* **2021**, *13*, 1597. [CrossRef]
25. Kumar, M.R.A.; Pu, J.H.; Hanmaiahgari, P.R.; Lambert, M.F. Insights into CFD modelling of water hammer. *Water* **2023**, *15*, 3988. [CrossRef]
26. Burgos-Méndez, Ó.J.; Coronado-Hernández, O.E.; Ramos, H.M.; Arrieta-Pastrana, A.; Pérez-Sánchez, M. Water hammer mitigation using hydro-pneumatic tanks: A multi-criteria evaluation of simulation tools and machine learning modelling. *Water* **2025**, *17*, 1883. [CrossRef]
27. Park, J.S.; Nguyen, Q.K.; Lee, G.N.; Jung, K.H.; Park, H.; Suh, S.B. Evaluation of water hammer for seawater treatment system in offshore floating production unit. *Processes* **2020**, *8*, 1041. [CrossRef]
28. Kim, N.-S.; Jeong, Y.-H. An investigation of pressure build-up effects due to check valve's closing characteristics using dynamic mesh techniques of CFD. *Ann. Nucl. Energy* **2021**, *152*, 107996. [CrossRef]

Disclaimer/Publisher's Note: The statements, opinions and data contained in all publications are solely those of the individual author(s) and contributor(s) and not of MDPI and/or the editor(s). MDPI and/or the editor(s) disclaim responsibility for any injury to people or property resulting from any ideas, methods, instructions or products referred to in the content.